AD-A276 352

NAVAL POSTGRADUATE SCHOOL
Monterey, California

THESIS

WAVEFORM GENERATION FOR
ULTRA-WIDEBAND RADAR SYSTEM

by

Chiang Hsiao-Feng

December 1993

Thesis Advisors: Gurnam. Gill
Darwish. A. A. Mohamed

Approved for public release; distribution is unlimited.

94-06800

94 3 01 025

1. AGENCY USE ONLY (Leave blank)	2. REPORT DATE December 1993	3. REPORT TYPE AND DATES COVERED Master's Thesis, Oct. 92 - Sept. 93

4. TITLE AND SUBTITLE WAVEFORM GENERATION FOR ULTRA-WIDEBAND RADAR SYSTEM	5. FUNDING NUMBERS

6. AUTHOR(S)

Chiang, Hsiao-Feng

7. PERFORMING ORGANIZATION NAME(S) AND ADDRESS(ES) Naval Postgraduate School Monterey, CA 93943-5000	8. PERFORMING ORGANIZATION REPORT NUMBER

9. SPONSORING/MONITORING AGENCY NAME(S) AND ADDRESS(ES)	10. SPONSORING/MONITORING AGENCY REPORT NUMBER

11. SUPPLEMENTARY NOTE

The views expressed in this thesis are those of the author and do not reflect the official policy or position of the Department of Defense or the United States Government.

12a. DISTRIBUTION/AVAILABILITY STATEMENT Approved for public release; Distribution is unlimited.	12b. DISTRIBUTION CODE

13. ABSTRACT (Maximum 200 words)

In the current literature, ultra-wideband (UWB) waveforms are said to possess several potential advantages such as penetration of foliage, walls and ground, as well as target identification and detection of stealth targets. Due to the potential advantages of UWB waveforms, UWB power sources are currently being developed. This thesis investigates the Fourier synthesis method of waveform generation which is to be used with ultra-wideband radar. The major advantages of this method over traditional methods are that accurate control of pulse shapes and pulse repetition intervals (PRI) can be generated. In this thesis, the Fourier method is extended to generation of binary coded waveforms for UWB systems. The generation of such codes is important as it allows for the use of longer coded pulses. These coded pulses contain more energy and improve signal to noise ratio (SNR) while still retaining the range resolution and other benefits of smaller pulse widths.

14. SUBJECT TERMS Ultra-wideband (UWB), Fourier Series Expansion, Fourier Synthesis, Continuous Wave Coded Waveform, Pulsed Coded Waveform.	15. NUMBER OF PAGES 87
	16. PRICE CODE

17. SECURITY CLASSIFICATION OF REPORT UNCLASSIFIED	18. SECURITY CLASSIFICATION OF THIS PAGE UNCLASSIFIED	19. SECURITY CLASSIFICATION OF ABSTRACT UNCLASSIFIED	20. LIMITATION OF ABSTRACT UL

WAVEFORM GENERATION FOR
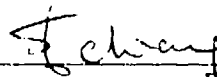ULTRA-WIDEBAND RADAR SYSTEM

by

Chiang Hsiao-Feng
Commander, The Republic of China Navy
B.S., Chung Cheng Institute of Technology, 1977

Submitted in partial fulfillment
of the requirements for the degree of
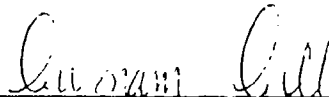
MASTER OF SCIENCE IN ELECTRICAL ENGINEERING

from the

NAVAL POSTGRADUATE SCHOOL
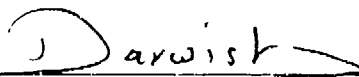December 1993

Author: _____
Chiang Hsiao-Feng

Approved by: _____
Gurnam Gill, Thesis Advisor

_____
Darwish Abdel Aziz Mohamed, Thesis Co-Advisor

_____
Michael Morgan, Chairman,
Department of Electrical and Computer Engineering

ii

ABSTRACT

In the current literature, ultra-wideband (UWB) waveforms are said to possess several potential advantages such as penetration of foliage, walls and ground, as well as target identification and detection of stealth targets. Due to the potential advantages of UWB waveforms, UWB power sources are currently being developed. This thesis investigates the Fourier synthesis method of waveform generation which is to be used with ultra-wideband radar. The major advantages of this method over traditional methods are that accurate control of pulse shapes and pulse repetition intervals (PRI) can be generated. In this thesis, the Fourier method is extended to generation of binary coded waveforms for UWB systems. The generation of such codes is important as it allows for the use of longer coded pulses. These coded pulses contain more energy and improve signal to noise ratio (SNR) while still retaining the range resolution and other benefits of smaller pulse widths.

iii

TABLE OF CONTENTS

LIST OF FIGURES

ix

I. INTRODUCTION

In recent years progress has been made in the development of ultra-wideband (UWB) technology. As a result, experimental UWB radars are being built and system concepts are being studied. UWB signals have special features which are not present in conventional radar waveforms. The feature is the presence of low frequency components and a very large bandwidth (or narrow pulse width) at the same time. The low frequency components may excite target resonances and penetrate ground and foliage. This may allow detection of low RCS targets at medium ranges including the detection of target' hidden in foliage or underground. Very narrow pulse widths give fine range resolution with a low amount of clutter. Decreased clutter is an important aspect of low RCS target detection.

The object of this thesis is to review and investigate the advances in generation of UWB waveforms. In chapter II of this thesis, the characteristics and theoretical aspects of UWB system are briefly introduced. Chapter III provides a review of the traditional method of UWB (impulse) waveform generation. The key concept behind the traditional impulse generation is the storage and compression of energy. Energy is stored from a continuous low power source for a period of time, to the capacity of the storage method or to the level

needed. The energy is then released in a very short period of time to obtain a high peak power. This process allows for the production of very high peak power of short duration from supplies with lower power. Chapter IV explains the method of waveform generation by the Fourier synthesis method. From Fourier theory, any periodic signal can be decomposed into the sum of its weighted sinusoids. Conversely, a periodic signal can be generated by a suitably weighted sum of sinusoids. Thus, any periodic waveform can be synthesized by summing the outputs of several harmonically related oscillators. Chapter IV extends the waveform generation beyond simple periodic pulses to the generation of complex amplitude coded waveforms. This capability will allow pulse compression and coherent integration of UWB signals which reduces the need for very large power sources as required for conventional impulse implementation. The last chapter presents the summary and the conclusions.

II. ULTRA-WIDEBAND SYSTEM

The ultra-wideband (UWB) system differs from conventional systems in that its bandwidth is a significant fraction of its center frequency. A typical narrow band radar may have bandwidth of 1 MHz centered at 1 GHz whereas a UWB radar may have instantaneous bandwidth extending from 200 MHz to 5 GHz. This extraordinarily large bandwidth has the potential of identifying targets, reducing the effectiveness of low-observable treatments and detecting targets in foliage or behind walls. These tasks are now considered difficult using current conventional narrow band systems. [Ref. 1:p. 371]

A.   DEFINITION OF ULTRA-WIDEBAND

Ultra-wideband (UWB) became an accepted electronic term after the 1990 Ultra-wideband conference in Los Alamos, New Mexico. UWB is defined as a signal whose bandwidth is at least wider than 25% of its center frequency. [Ref. 1:p. 371]

Conventionally, the bandwidth of a signal is described in terms of its frequency spread called absolute bandwidth (BW) (defined as the value between the highest and the lowest frequencies of interest in the signal). The center frequency is defined as the middle of this frequency spread. [Ref. 2:p. 464] These relationships can be expressed in the form of equations as

$$\text{absolute bandwidth (BW)} = f_h - f_l ,$$

$$\text{center frequency } (f_c) = \frac{f_h + f_l}{2} , \qquad (2.1)$$

where

f_h is the highest frequency of interest in the signal,

f_l is the lowest frequency of interest in the signal,

f_c is the center frequency of the signal.

Another way to express bandwidth is called relative bandwidth (η). Relative bandwidth is the ratio of frequency spread to the center frequency of the signal. [Ref. 3:P. 19-21]

$$\text{relative bandwidth } (\eta) = \frac{f_h - f_l}{f_c} \times 100$$

$$= \frac{2 \cdot (f_h - f_l)}{f_h + f_l} \times 100 . \qquad (2.2)$$

Relative bandwidth (η) is thus equal to or greater than 25% for UWB signals. Larger relative bandwidths can be achieved by the generation of a pulse containing one or few cycles of a sinusoidal carrier or by the generation of narrow baseband pulses. [Ref. 4:p. 486]

B.   WAVEFORM AND FREQUENCY SPECTRUM

In this section, the bandwidth of the radar signal generated by transmitting few cycles of the carrier is derived. [Ref. 5:p. 4-5]

4

A time waveform $s(t)$ has a frequency spectrum $S(f)$ given by its Fourier transform

$$S(f) = \int_{-\infty}^{\infty} s(t) \cdot e^{-j2\pi ft} dt \ . \tag{2.3}$$

If $s(t)$ is a pulsed signal consisting of a sinusoid of frequency f_0 and duration τ, then equation (2.3) becomes

$$S(f) = \int_{-\frac{\tau}{2}}^{\frac{\tau}{2}} \sin(2\pi f_0 t) \cdot e^{-j2\pi ft} dt \tag{2.4}$$

$$= \frac{j\tau}{2} \cdot \left[\frac{\sin[\pi(f_0+f)\tau]}{\pi(f_0+f)\tau} - \frac{\sin[\pi(f_0-f)\tau]}{\pi(f_0-f)\tau} \right] \ .$$

Since a pulse of duration τ contains N cycles, then τ is equal to N/f_0. Substituting N/f_0 for τ in the above equation, one obtains the magnitude of $S(f)$ as

$$|S(f)| = \frac{1}{\pi f_0} \cdot \left| \frac{\sin\left(N\pi\frac{f}{f_0}\right)}{1-\left(\frac{f}{f_0}\right)^2} \right| \ . \tag{2.5}$$

Spectra for pulses consisting of different numbers of cycles of sine wave are shown in Figure (2.1). This figure shows that the spectrum is not symmetrical about the center frequency f_0 when N is small.

Table (2.1) gives f_m, f_l, f_h and relative bandwidth for the number of cycles, N, of the carrier in a pulse. N varies from 1 to 9,
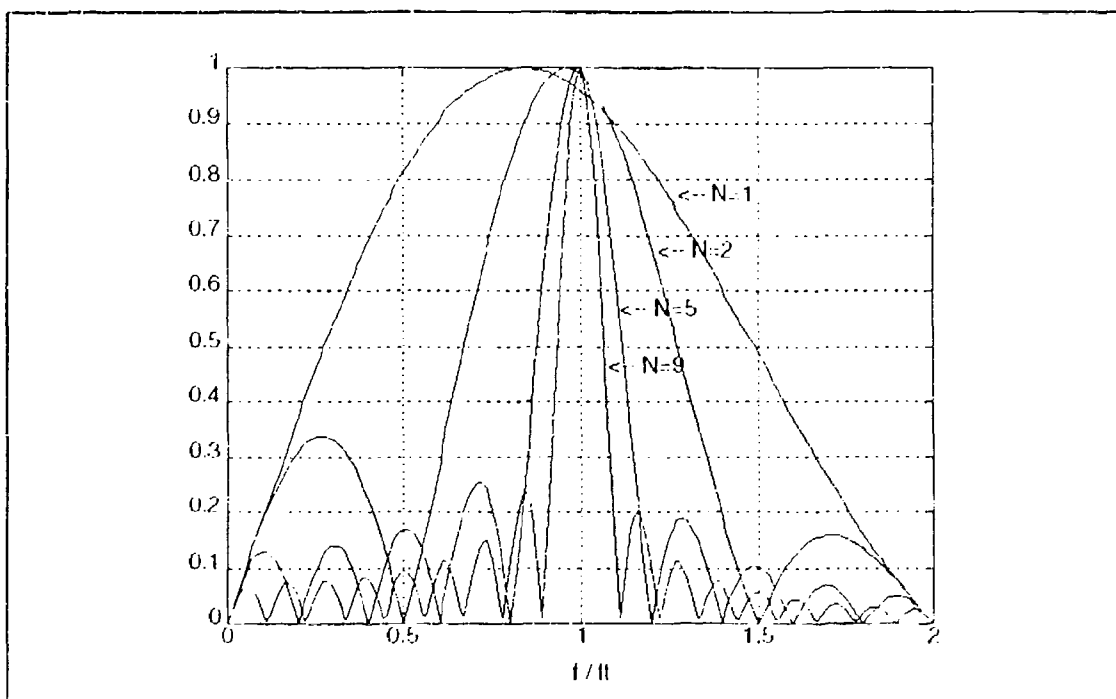
Figure 2.1   Frequency spectrum of N cycle sine wave

where

f_l is the lower 3dB frequency,

f_h is the higher 3dB frequency,

f_m is the frequency of peak amplitude,

η, the relative bandwidth is calculated from 3dB bandwidth.

TABLE 2.1   RELATIVE BANDWIDTH FOR SINUSOIDAL WITH NUMBER OF CYCLES (N) FROM 1 TO 9

	N=1	N=2	N=3	N=4	N=5	N=6	N=7	N=8	N=9
f_m/f_l	0.84	0.96	0.98	0.99	0.99	1.00	1.00	1.00	1.00
f_l/f_l	0.42	0.75	0.84	0.89	0.91	0.93	0.94	0.95	0.95
f_h/f_l	1.30	1.18	1.13	1.10	1.08	1.07	1.06	1.05	1.04
η	88%	43%	29%	21%	17%	14%	12%	10%	9%

6

The value of f_m is determined by $S(f_{max})$, the values of f_l and f_h are calculated by solving

$$|S(f)| = \frac{|S(f_{max})|}{\sqrt{2}} , \qquad\qquad (2.6)$$

where

    $S(f)$ is given by equation (2.5),

    $S(f_{max})$ is the maximum value of equation (2.5).

From Table (2.1), one may conclude that a signal will not be a UWB signal according to the definition unless it has three or fewer cycles of carrier in its waveform.

C.   CHARACTERISTICS OF ULTRA-WIDEBAND WAVEFORM

As mentioned earlier, ultra-wideband signals have two major distinguishing characteristics as compared to conventional narrow band signals. UWB signals have very wide bandwidths and contain low frequency components. Some implications of these characteristics are as follows.

1.   Implications of Very Wide Bandwidth

a.   Fine Range Resolution

The range resolution is determined by the following relationship:

$$\text{Range resolution} = \frac{c\,\tau}{2} \approx \frac{c}{2B} , \qquad\qquad (2.7)$$

where

    c is speed of light,

    τ is pulse width,

B is bandwidth, usually approximated as $1/\tau$.

This relationship shows that the UWB system has improved range resolution due to the increased bandwidth.

b. Low Clutter

Small resolution cell size (due to small pulse width) reduces the clutter power contained in a single range cell, leading to better detection performance in the presence of a large amount of clutter. [Ref. 6:p. 1]

c. High Sampling Rate and Extensive Signal Processing

If digital processing is used, sampling rates will increase with bandwidth and consequently signal processing will increase proportionally.

2. Implications of Low Frequency Component

a. Propagation and Penetration Ability

Low frequencies will attenuate slower than high frequency components during propagation in any medium. So, one can expect increased ground penetration and foliage penetration.

b. Low Radar Cross Section (RCS) Target Detection

At low frequencies the negligibly small rain or cloud echoes will not seriously interfere with the detection of desired targets. [Ref 7:p. 193]

D.   POTENTIAL APPLICATIONS

1.   Foliage Penetration

Foliage penetration capabilities result from combining a long wavelength with a wide bandwidth. The long wavelength contributes to penetration ability by decreasing the backscatter coefficient from trees, while the wide bandwidth preserves the high resolution that would otherwise be lost by going to lower frequencies.

2.   Ground Penetration

Ground penetration radars take advantage of low absorption from soils at low frequencies and strive to maintain resolution by using larger bandwidths (or shorter pulse widths). In ground-penetration radar designs, it is common practice to use 100% relative bandwidth (for example operating the frequency between 50 MHz and 150 MHz). The transmitted waveform is often close to a single cycle and is derived from a singly-switched impulse.

3.   Target Identification

High-resolution radar technology at X-band is a proven design capable of providing range resolution below one meter. UWB systems can provide even better range resolutions because they utilize very short pulses. The potential of this ultra-high range resolution allows targets to be resolved into individual scattering centers and thereby enhance target identification. [Ref. 1:P. 373]

III. TRADITIONAL HIGH VOLTAGE PULSE GENERATION

Signal waveform is an important part of radar design. Given other parameters, the energy of the pulse determines detection performance. A traditional method of generating a pulse train is by using a switch that is connected to a power source and a load. By turning the switch "on" and "off", a pulse train is generated. The requirements of UWB signal waveforms include high power, a fast rise time, and the ability to generate waveforms with precision. This chapter deals with the basic concept and devices used in the generation of high voltage waveforms.

A. BASIC CONCEPT

The basic concept of generating a high voltage short duration pulse is shown in Figure (3.1). The rise time of the pulse is determined by the impedance of an energy storage circuit, the load impedance, and the resistive and inductive characteristics of the switch and the switch circuit geometry. [Ref. 5:P. 11]

When the switch is open, the current from the energy source charges the energy storage capacitor (C) through the charging impedance (R), and the voltage across the energy storage capacitor builds up with time as given by the following equation, [Ref 8:p. 111-120]
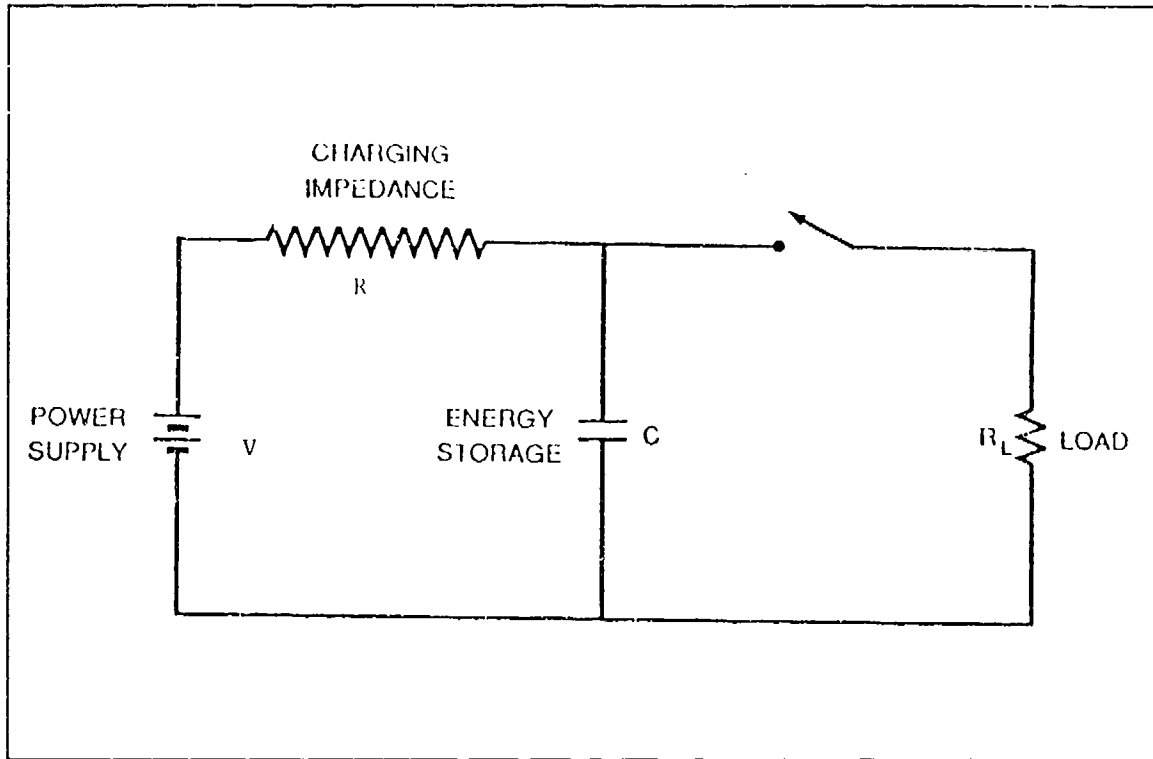
Figure 3.1   Basic principle of the pulse generator
                [From Ref. 5:p. 12]

$$V_c(t) = V - V \cdot e^{\frac{-t}{RC}} = V \cdot \left(1 - e^{\frac{-t}{RC}}\right) \; . \qquad (3.1)$$

Closing the switch allows the stored energy in the capacitor to discharge rapidly through the load. The charging impedance (R) is much larger than the load impedance (R_L). The discharge voltage as given by the equation [Ref 8:p. 111-120]

$$V_c(t) = V_{c\,max} \cdot e^{\frac{-t}{RC}} \; . \qquad (3.2)$$

By switching on and off at certain intervals, the capacitor is charged and discharged resulting in a train of pulses. The duration of the discharge pulse is inversely

11

proportional to the load impedance (R_L) and the capacitance (C). The rise and fall times depend mostly on the characteristics of the switching process. A transmitter must be able to provide a short rise and fall time in order to generate a pulse approximating the ideal impulse.

B.   SWITCHING DEVICES

The switching device is the means by which a nonconducting medium becomes conductive. There are different types of switches, to include "spark gap" [Ref. 9:p. 529-537], "photoconductive" [Ref. 10:p. 124-126] and [Ref. 11:p. 266-271], "hydrogen thyratron" [Ref. 12:p. 256-265], "high pressure gas" [Ref. 13:p. 277-282], "air break down tail erosion" [Ref. 14:p. 283-298], and "gas avalanche" [Ref. 15:p. 299-315], etc. They all are claimed to be able to meet the UWB waveform requirement. The most basic and popular are the "spark gap" and "photoconductive" types of switching.

1.   Spark Gap Switching Device

The spark gap switching device used in the UWB system is also known as the Hertzian generator. A Hertzian generator diagram is shown in Figure (3.2). Its operation can be described as follows: a 50 KV power supply is fed through a 200 MΩ resistor and charges the capacitor until some nominal value, e.g., 10 KV, appears across the pressurized spark gap. If the spark gap is adjusted to fire at 10 KV, it will break down the plasma between the points and the arc. At that

12
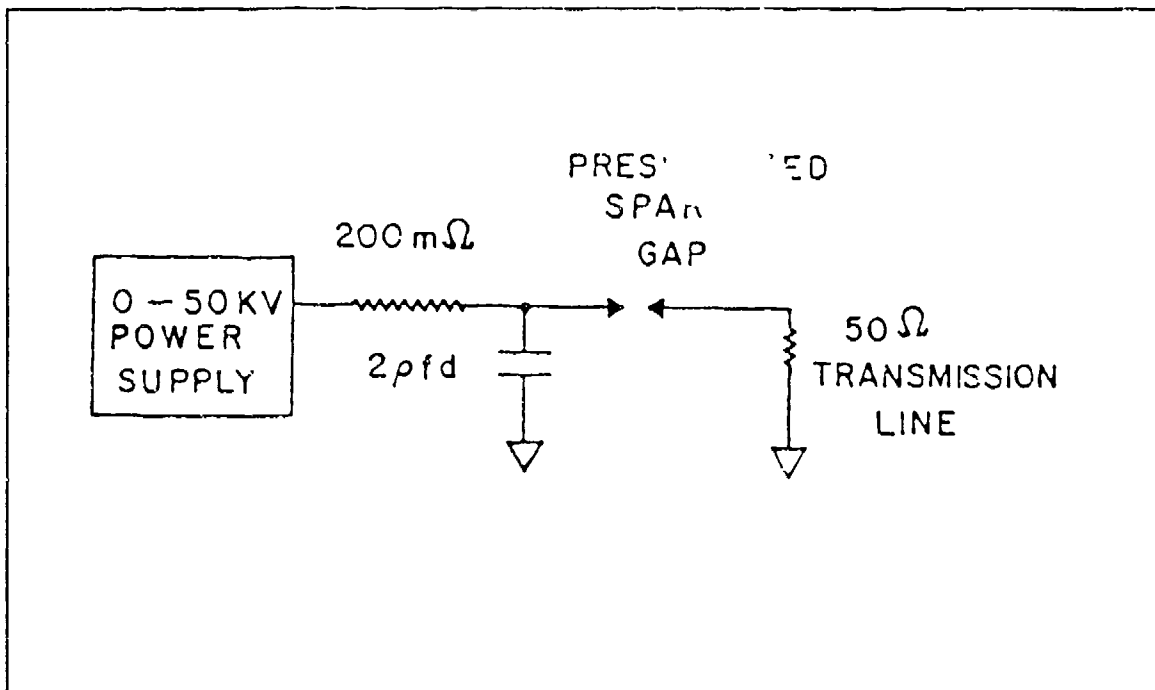
Figure 3.2   Diagram of a typical Hertzian impulse
                  generator [From Ref. 16:p. 539]

instant, the resistance is very low and the mechanism can be
considered to physically be a switch in the closed position.
The 10 KV across the 2 picofarad capacitor then discharges
into the 50 Ω transmission line. After the capacitor
discharges, the plasma disappears and the capacitor will
charge again through the 200 MΩ resistor. This self-generating
pulse repetition frequency (PRF) is determined by the R-C time
constant. The optimum results are determined by geometry
configuration and gap spacing. [Ref. 16:P. 535]

2.   Photoconductive Switching Device

Photoconductive switches are optically controlled
devices. The conductivity of the semiconductor material is
proportional to the total photon flux illuminating this
material. When illuminated by the laser, the energy of the

laser photons exceeds the band gap energy of the semiconductor. Electrical carriers are created by photons absorbed in a semi-insulating or high resistivity semiconductor material causing the material to change from its highly resistive state into a highly conductive state. This material conducts until illumination is ended. If this change in conductivity is sufficiently strong and fast, the device acts like a switch. Switching speed is the greatest advantage of the photoconductive switching device. The generation time necessary to absorb a photon and liberate an electron-hole pair is on the order of 10^{14} seconds.

C. ENERGY STORAGE DEVICE

The output pulse from the primary energy storage method described in Figure (3.1) has too low of a voltage for UWB system applications. In these cases the primary pulse is frequently sent through a voltage-multiplier circuit. The most common voltage-multiplier circuit, especially at high energy levels, is the Marx generator. A basic Marx circuit is shown in Figure (3.3). This circuit is basically a number of N capacitor stages charged in parallel to some voltage V and then connected in series by a number of N switches to discharge and produce an output voltage NV. The number of stages is dependent upon the input voltage available and the required output voltage and power.

The problem with this traditional high voltage pulse

14
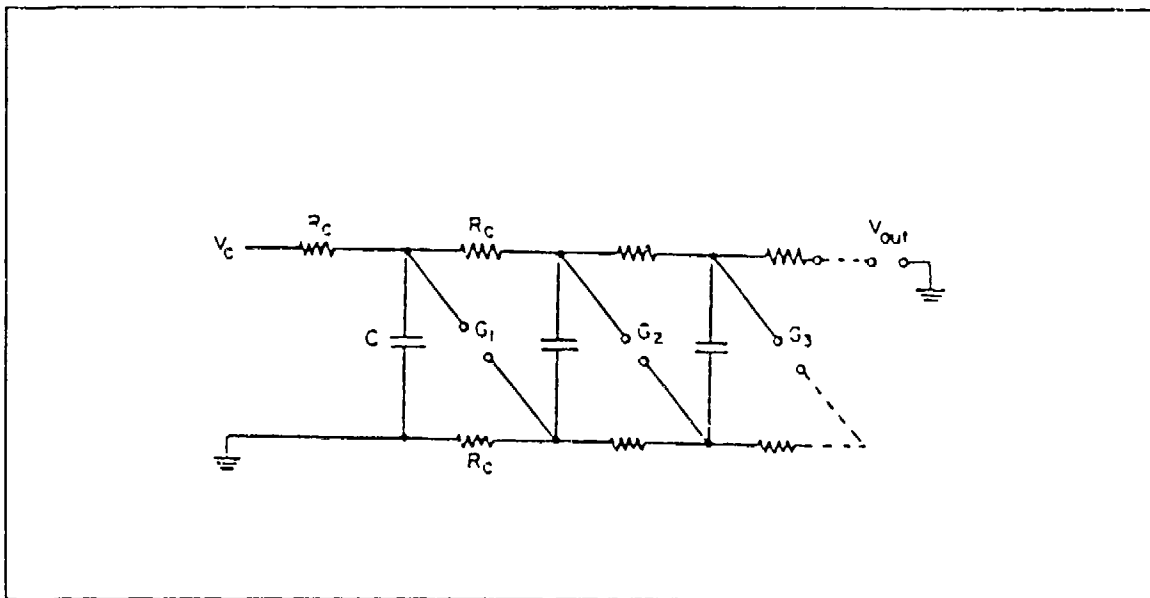
Figure 3.3   Basic Marx circuit
               [From Ref. 17:p. 415]

generator is that a significant amount of energy lies around the dc component. The antenna acts like a high pass filter and does not radiate dc and thus this kind of narrow pulse generator is not efficient for radiation. Another disadvantage is that the pulse shape and PRI are not well controlled. There is no fine control of spectrum to avoid interference with friendly receivers. All these problems can be avoided by using the Fourier method of waveform generation which is discussed in the next chapter.

IV. FOURIER SYNTHESIS OF WAVEFORMS

From Fourier theory, any periodic signal can be decomposed into a sum of weighted sinusoids. Conversely, a periodic signal can be generated by a suitably weighted sum of sinusoids. Thus, any periodic waveform can be synthesized by summing the outputs of several harmonically related oscillators. This chapter extends the waveform generation beyond simple periodic pulse waveforms. Generation of waveforms with complicated amplitude codes will be described. By Fourier synthesis, a variety of coded waveforms can be generated with accurate control of pulse shapes and pulse repetition intervals (PRI).

A. BASIC CONCEPT OF FOURIER SYNTHESIS OF WAVEFORMS

From Fourier theory, any periodic function of time $x(t)$ can be expressed as a linear combination of a constant a_0 plus all the sine and cosine functions whose frequencies are integer multiples of the fundamental frequency (f_0).

$$x(t) = \frac{a_0}{2} + \sum_{n=1}^{\infty} \left[a_n \cdot \cos(nw_0 t) + b_n \cdot \sin(nw_0 t) \right] , \qquad (4.1)$$

where

n is an integer,

T is period,

$f_0 = 1/T$,

$$w_0 = 2 \cdot \pi \cdot f_0,$$

and a_0, a_n, and b_n are Fourier coefficients, as follows

$$a_0 = \frac{2}{T} \int_{-\frac{T}{2}}^{\frac{T}{2}} x(t) \, dt ,$$

$$a_n = \frac{2}{T} \int_{-\frac{T}{2}}^{\frac{T}{2}} x(t) \cdot \cos(nw_0 t) \, dt , \qquad (4.2)$$

$$b_n = \frac{2}{T} \int_{-\frac{T}{2}}^{\frac{T}{2}} x(t) \cdot \sin(nw_0 t) \, dt .$$

For the equation (4.1), the second term on the right-hand side is the summation of an infinite number of harmonics which are practically impossible to achieve. Mathematically this can be separated into a finite sum and an infinite sum.

$$x(t) = \frac{a_0}{2} + \sum_{n=1}^{N} [a_n \cdot \cos(nw_0 t) + b_n \cdot \sin(nw_0 t)]$$

$$\qquad (4.3)$$

$$+ \sum_{n=N+1}^{\infty} [a_n \cdot \cos(nw_0 t) + b_n \sin(nw_0 t)] .$$

Allowing the sum of the first 2N+1 terms to be the Fourier series representation for $x(t)$, the sum of the rest of the terms can be listed as an error. The constant N is an integer which makes the error reasonable and acceptable. Then $x(t)$ can be approximated as

$$x(t) \approx \frac{a_0}{2} + \sum_{n=1}^{N} [a_n \cdot \cos(nw_0 t) + b_n \cdot \sin(nw_0 t)] . \qquad (4.4)$$

17

The above equation can be used to generate $x(t)$ by simultaneously transmitting all of the N frequency components of $x(t)$. When using a stable source for each spectral component and coherently transmitting these signals through a wideband antenna, an $x(t)$ is formed in space where $x(t)$ is any function which can be Fourier analyzed. For normal radar functions, $x(t)$ is usually a train of pulses. This approach differs from the previous methods which generate the short pulses in real time by switching the signal on and off quickly.

Since radiated waveforms do not contain a dc component, a_0 can be made to be equal to zero. This allows the equation (4.4) to be written as

$$x(t) = \sum_{n=1}^{N} \left[a_n \cdot \cos(nw_0 t) + b_n \cdot \sin(nw_0 t) \right] . \qquad (4.5)$$

B.   FOURIER SYNTHESIS FOR SIMPLE PULSE WAVEFORMS

1.   Fourier Series Method

Consider a simple rectangular pulse train, see Figure (4.1a). Each rectangular pulse has amplitude A and width τ. The pulse train can be mathematically described as

$$x(t) = A \cdot \sum_{n=-\infty}^{\infty} \Pi(t - nT - t_0) , \qquad (4.6)$$

18
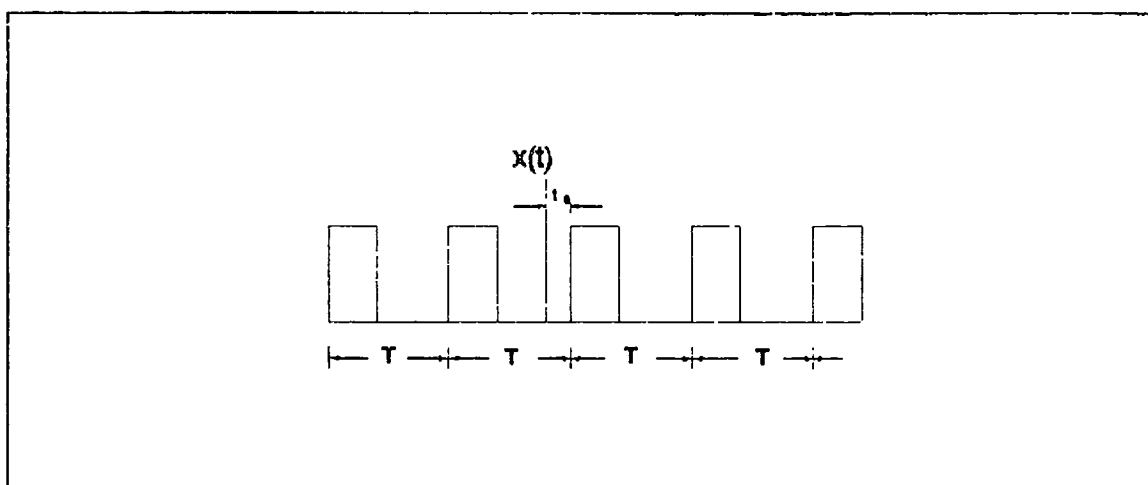
Figure 4.1a   Simple rectangular pulse train

where

t_0 is the time shift,

$$\Pi(t) = \begin{cases} 1, & 0 < t < \tau ; \\ 0, & \tau < t < T . \end{cases}$$

From equation (4.2), one can calculate the Fourier coefficients a_n and b_n as follows

$$a_n = \frac{2}{T} \cdot \int_{t_0}^{t_0+\tau} A \cdot \cos(nw_0 t)\, dt$$

$$= \frac{2A}{n\pi} \cdot \sin\left[\frac{nw_0 \tau}{2}\right] \cdot \cos\left[nw_0\left(t_0 + \frac{\tau}{2}\right)\right],$$

$$b_n = \frac{2}{T} \cdot \int_{t_0}^{t_0+\tau} A \cdot \sin(nw_0 t)\, dt \tag{4.7}$$

$$= \frac{2A}{n\pi} \cdot \sin\left[\frac{nw_0 \tau}{2}\right] \cdot \sin\left[nw_0\left(t_0 + \frac{\tau}{2}\right)\right].$$

From equations (4.5) and (4.7), the train of pulses can be approximated as

$$x(t) \cong \sum_{n=1}^{N} \left[a_n \cdot \cos(nw_0 t) + b_n \cdot \sin(nw_0 t) \right]$$

$$= \frac{2A}{n\pi} \cdot \sum_{n=1}^{N} \left\{ \sin\left[\frac{nw_0 \tau}{2} \right] \cdot \cos\left[nw_0 \left(t_0 + \frac{\tau}{2} \right) \right] \cdot \cos(nw_0 t) \right. \tag{4.8}$$

$$\left. + 2\sin\left[\frac{nw_0 \tau}{2} \right] \cdot \sin\left[nw_0 \left(t_0 + \frac{\tau}{2} \right) \right] \cdot \sin(nw_0 t) \right\}.$$

Two examples illustrate the waveforms which are generated by equation (4.8). In the first example, the following parameters are used.

Time shift (t_0) = 0,

Amplitude (A) = 1,

PRF = 250 MHz,

Pulse width (τ) = 0.5 nanoseconds,

Number of harmonics (N) = 9.

$$x(t) - \frac{a}{n\pi} \cdot \sum_{n=1}^{N} \left[\sin(nw_0 \tau) \cdot \cos(nw_0 t) + 2\sin^2\left[\frac{nw_0 \tau}{2} \right] \cdot \sin(nw_0 t) \right]. \tag{4.9}$$

The corresponding waveform is shown in Figure (4.1b). In the second example, the number of harmonics is changed to 64 and the rest of the parameters remain the same. The corresponding waveform is shown in Figure (4.1c).

Figure 4.1b   Waveform generated by equation (4.8) with
               A=1, PRF=0.25 GHz, τ=0.5 nsec, t_0=0, N=9.
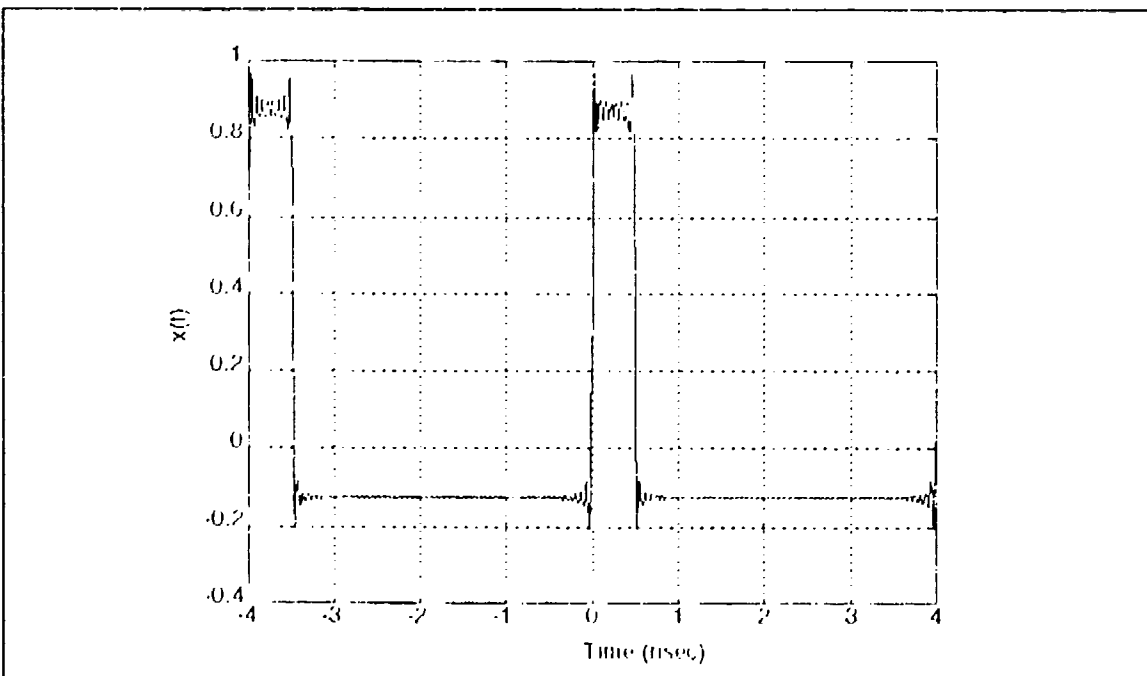
Figure 4.1c   Waveform generated by equation (4.8) with
               A=1, PRF=0.25 GHz, τ=0.5 nsec, t_0=0, N=64.

21

By looking at these two waveforms, one can see that the greater the number of harmonics, the more closely the pulse shape matches the desired pulse width (τ). Actually the pulse shape by itself is not of such great importance in radar waveform design, as long as a matched filter can be implemented for the transmitted waveform.

It may be easier to generate a periodic train of pulses if the Fourier series expansion is performed using symmetry (i.e., $t_0 = -\tau/2$ or $T - \tau/2$). The coefficients for the sine terms are zero.

$$x(t) \simeq \sum_{n=1}^{N} \left[\frac{2A}{n\pi} \cdot \sin\left(\frac{nw_0\tau}{2} \right) \cdot \cos\left(nw_0 t \right) \right]. \qquad (4.10)$$

In this case there will be only cosine terms in the expansion. This may simplify waveform generation. Using the same parameters as in previous examples, the corresponding waveforms generated by equation (4.10) are shown in Figures (4.2a) and (4.2b).

The waveforms generated by these two approaches are the same, as seen in Figures (4.1b), (4.1c), (4.2a) and (4.2b) but the latter may be more convenient.
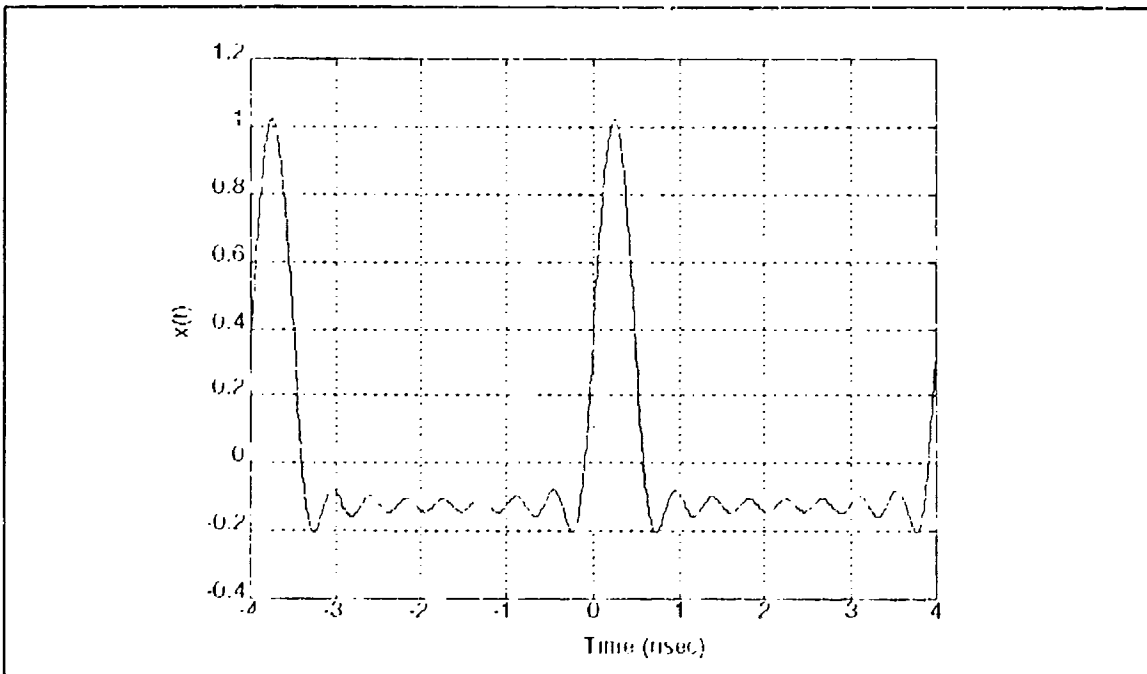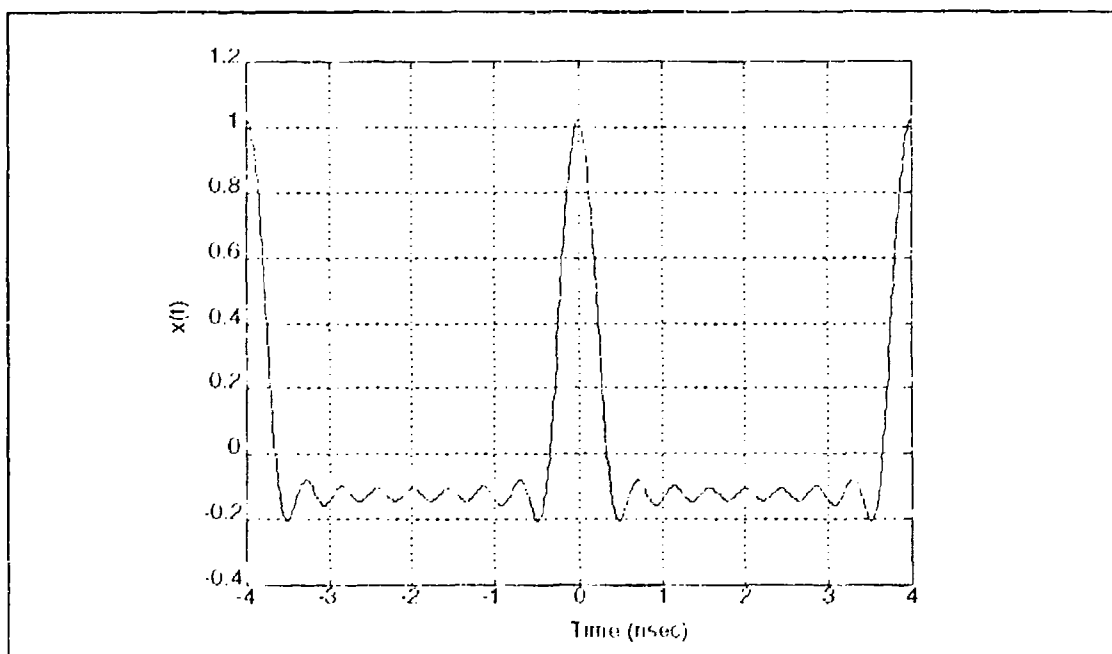
Figure 4.2a   Waveform generated by equation (4.8) with
A=1, PRF=0.25 GHz, τ=0.5 nsec, t_0=-τ/2, N=9.
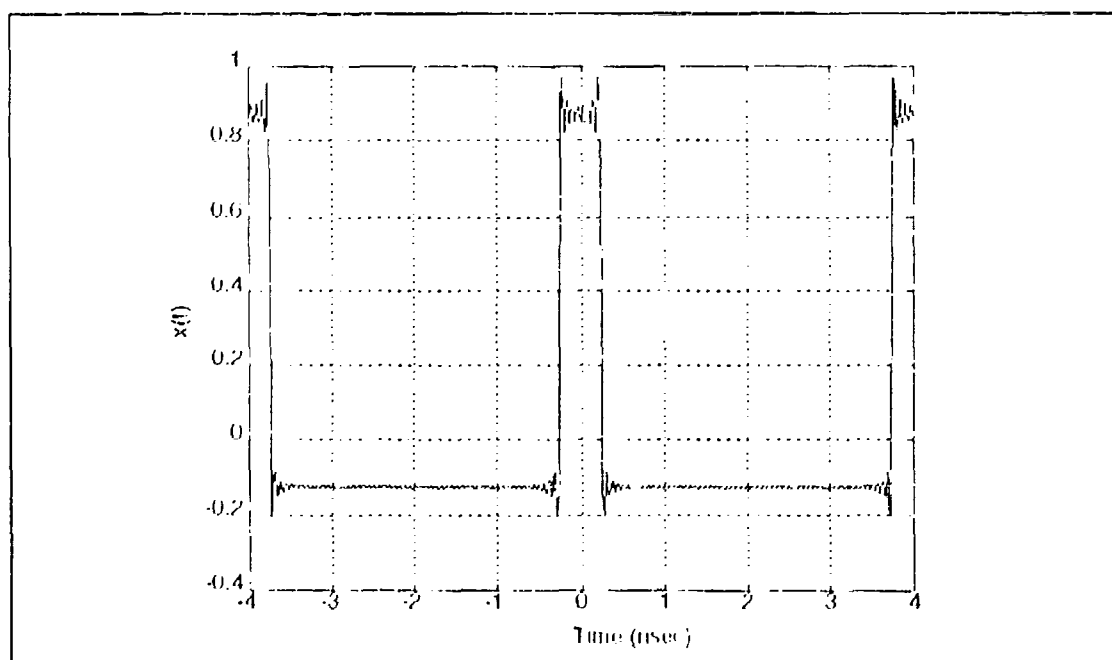
Figure 4.2b   Waveform generated by equation (4.8) with
A=1, PRF=0.25 GHz, τ=0.5 nsec, t_0=-τ/2, N=64.

23

2. Sum of Sinusoids Method

Another way to generate a narrow pulse is by summing up a number of sinusoids:

$$x(t) = \sum_{n=1}^{N} \cos(nw_0 t) .$$ (4.11)

Using the Euler's formula, equation (4.12) can be expressed in exponential form as:

$$x(t) = \sum_{n=1}^{N} \cos(2\pi n f_0 t) - \frac{1}{2} \cdot \sum_{n=1}^{N} \left(e^{j2\pi n f_0 t} + e^{-j2\pi n f_0 t} \right) .$$ (4.12)

Then, equations (4.12) can be written as:

$$
\begin{aligned}
x(t) &= \frac{1}{2} \left[\frac{1 - e^{j2\pi(N+1)f_0 t}}{1 - e^{j2\pi f_0 t}} - 1 + \frac{1 - e^{-j2\pi(N+1)f_0 t}}{1 - e^{-j2\pi f_0 t}} - 1 \right] \\
&= e^{j\pi N f_0 t} \cdot \frac{\sin[\pi(N+1)f_0 t]}{2\sin(\pi f_0 t)} + e^{j\pi N f_0 t} \cdot \frac{\sin[\pi(N+1)f_0 t]}{2\sin(\pi f_0 t)} - 1 \\
&= \frac{\sin(\pi N f_0 t)}{\sin(\pi f_0 t)} \cdot \cos[\pi(N+1)f_0 t] .
\end{aligned}
$$

(4.13)

The form of equation (4.13) is that of a slowly varying amplitude function multiplied by a sinusoidal signal $\cos(2\pi f_0 t)$. Figure (4.3) shows the amplitude function of the sinusoidal signal with PPF of 0.25 GHz and the number of harmonics used (N) equal to nine which explains that the pulse is formed by amplitude shaping of the sinusoid.

To compare the waveforms generated by Fourier series
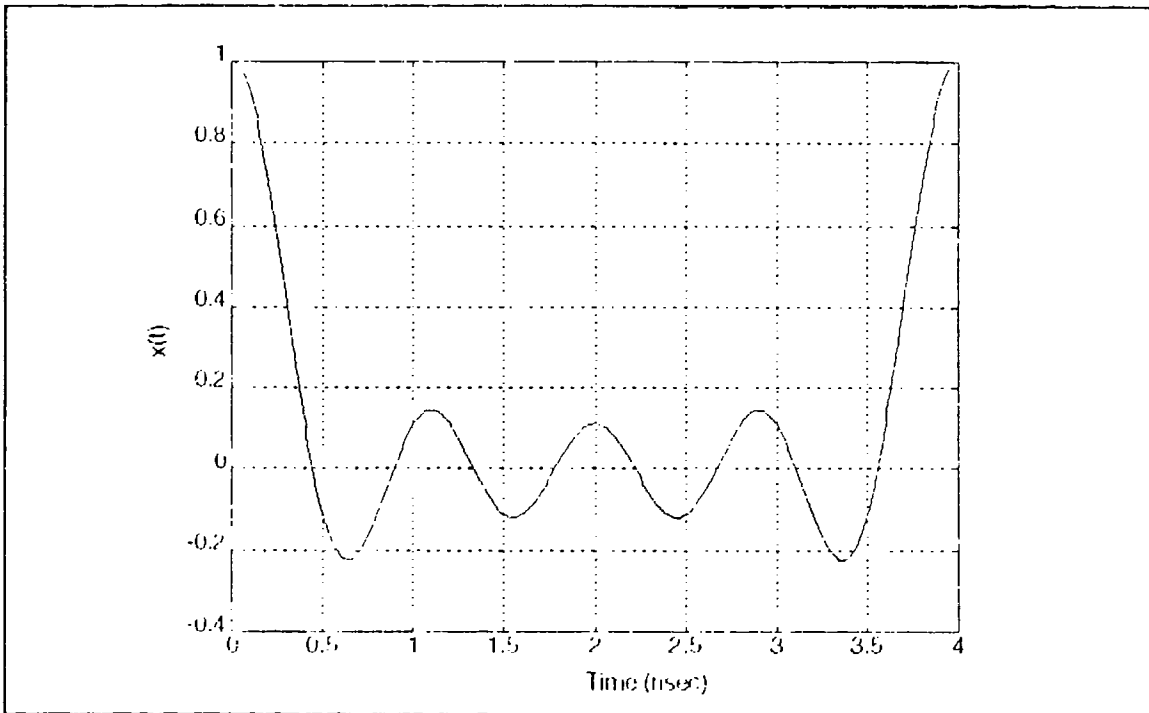
Figure 4.3   Amplitude function of equation (4.13) with
                    A=1, PRF=0.25 GHz, N=9.

method shown in Figure (4.2), the corresponding waveforms
generated by this method are shown in Figures (4.4a) and
(4.4b) for the fundamental PRF of 0.25 GHz and the number of
harmonics used equal to nine and 64. The resulting amplitude
has been normalized.

        From Figure (4.4), it can be seen that

  O   The number of harmonics greatly influences the width of
      a synthetic pulse. The greater the number of harmonics
      used, the narrower the pulse will be.

  O   The desired synthetic pulse width is a function of the
      fundamental PRF and the number of harmonics. The main
      lobe width measured between the lowest points is T/(N-1).
      In the case of Figure (4.4a), the period T is 4
      nanoseconds and the number of harmonics is nine, the
      synthetic pulse width is 0.5 nanoseconds.
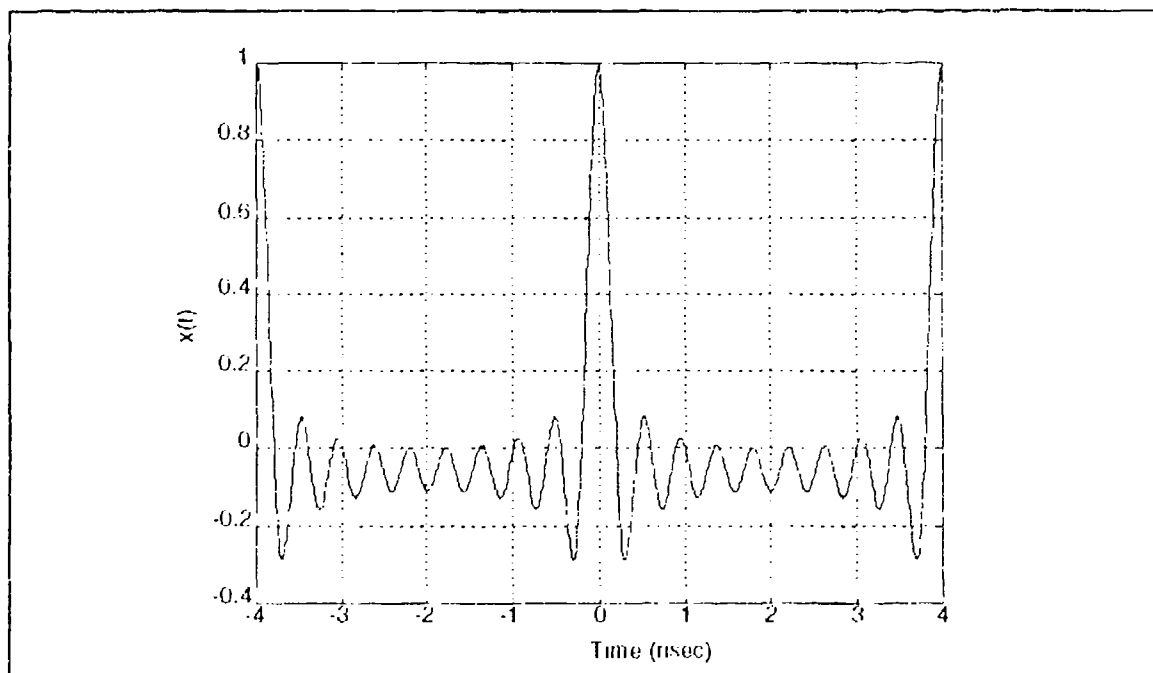
Figure 4.4a   Waveform generated by equation (4.12) with
                 A=1, PRF=0.25 GHz, N=9.
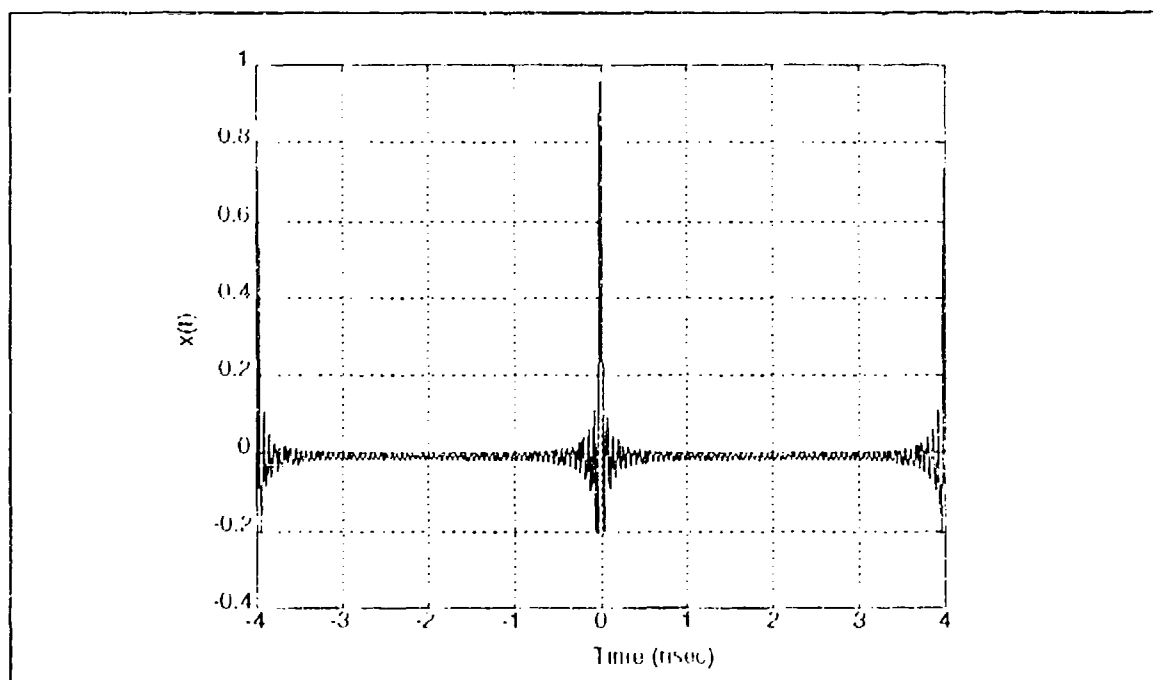
Figure 4.4b   Waveform generated by equation (4.12) with
                 A=1, PRF=0.25 GHz, N=64.

3. Implementation

As previously described, very short pulses can be generated by summing weighted or unweighted sinusoidal components. By using a stable source for each spectral component and coherently transmitting these signals through a wideband antenna which has a common phase center for all the spectral components, a train of short pulses can be formed. A block diagram of the transmitter is shown in Figure (4.5).
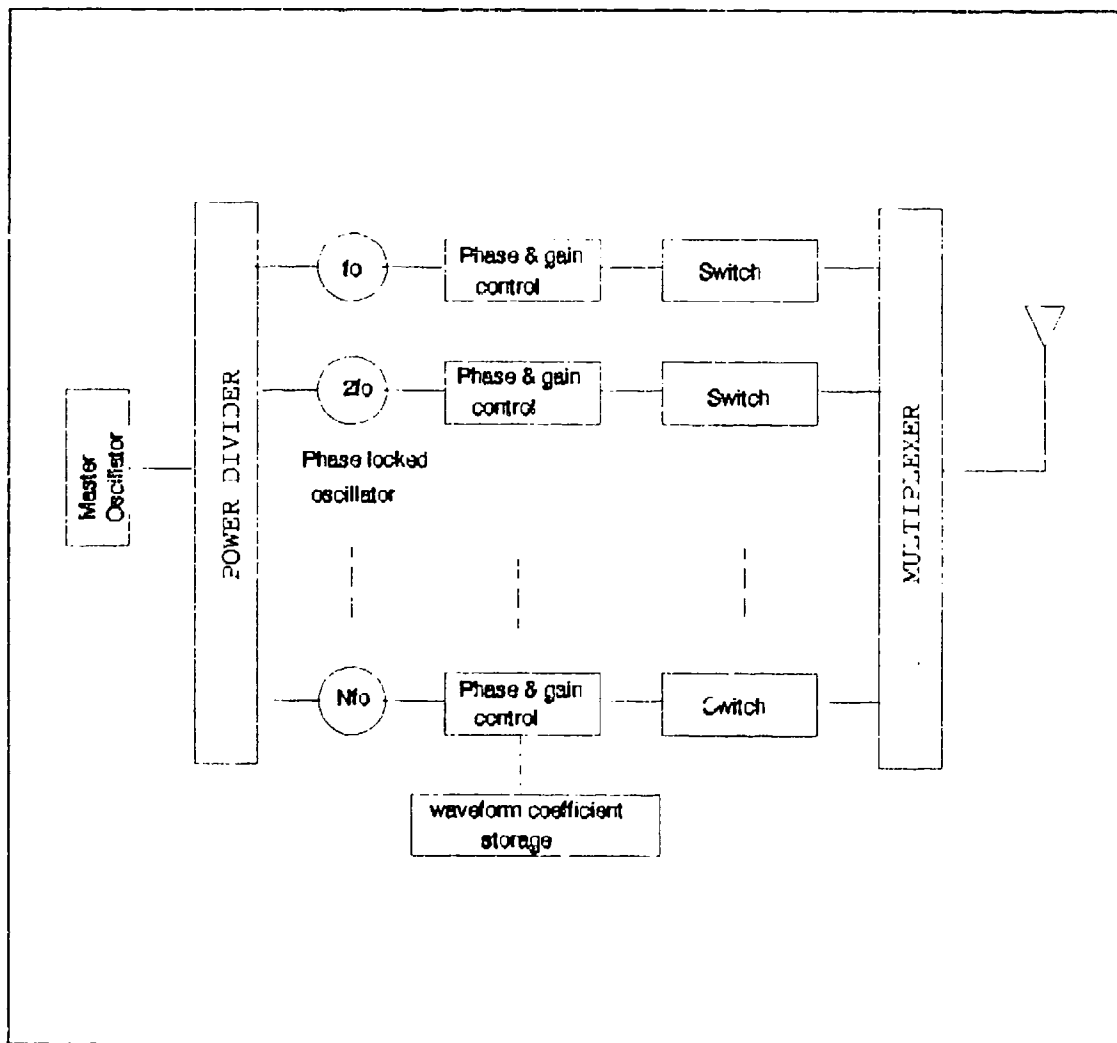
Figure 4.5   Block diagram of the transmitter

Frequency sources are generated by a bank of phase-locked oscillators. To phase-lock all the frequencies, a master oscillator is used as a reference. The frequency of this reference is the fundamental frequency. The phase-locked oscillator provides the required frequency accuracy, spectral purity, low noise and frequency stability. [Ref. 18:p. 127]

The dc component of the Fourier series cannot be transmitted and therefore is not included in the waveform generation. These factors limit the generated waveform to being an approximation of the ideal waveform. However if an antenna is properly designed, these "approximate" waveforms can be transmitted without dispersion where as an "ideal" rectangular waveform would be distorted by the antenna. In theory, these approximate waveforms actually may be superior to the ideal rectangular waveform. Power in the pulses goes up as the number of oscillators is increased. High-powered pulses can be generated by using many oscillators of lesser power. The choice of fundamental frequency (being the lowest frequency component) is important and its selection is based on its ground foliage penetration capability, target size, noise considerations (galactic and 1/f) and burst PRI.

Figure (4.6) shows the result from both methods. In a real system, either method can be used. The coefficients set for different waveforms can be precomputed and stored. When a particular waveform needs to be generated, corresponding coefficients will be used for amplitude modulation in

28
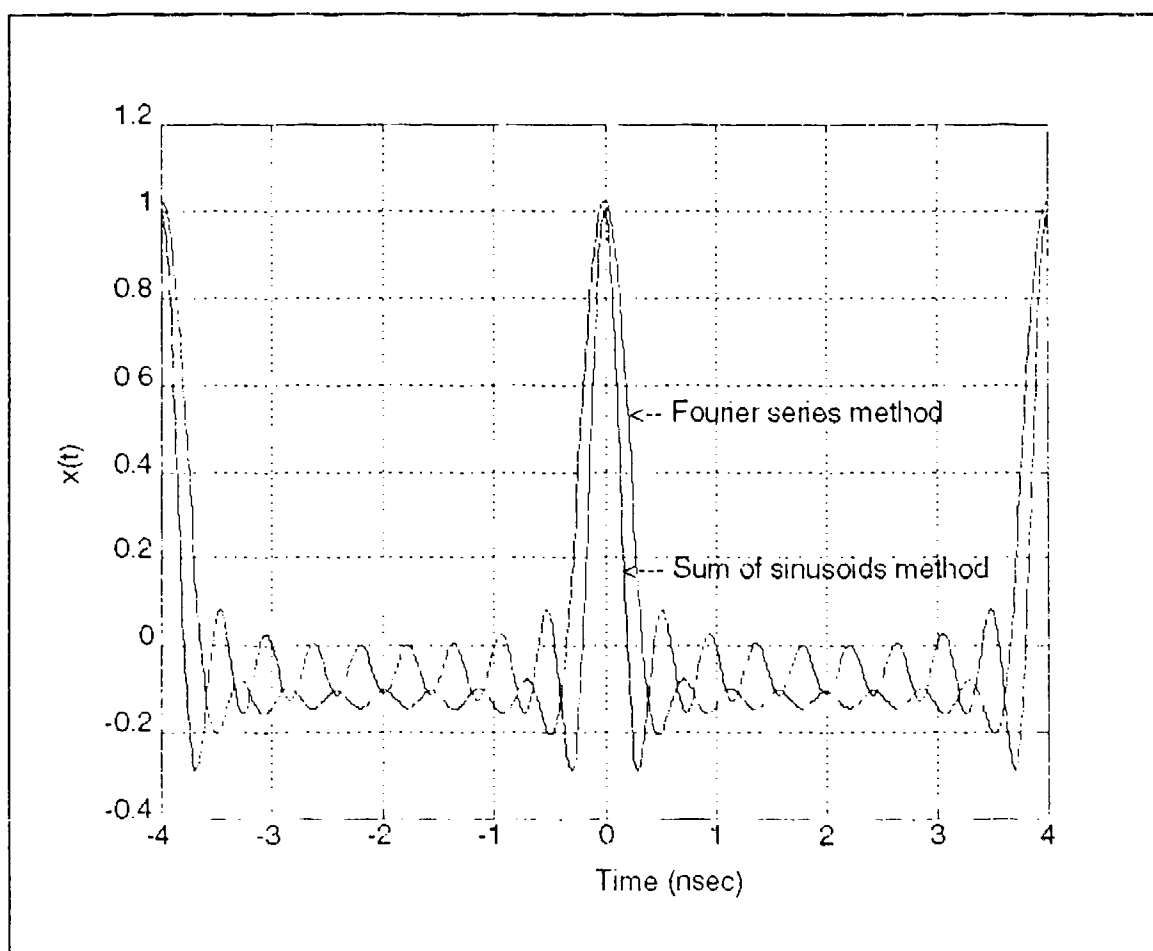
Figure 4.6   Waveform comparison for "Fourier series
              method" and "Sum of sinusoid method"

conjunction with the oscillators to produce the required
waveforms.

As discussed previously, the synthetic pulse width
is related to the number of harmonics and the fundamental
frequency. The pulse repetition frequency (PRF) is fixed by
f_0. A desired PRF can be controlled by an on-off switch.
Oscillators can be turned on at the beginning of the pulse and
turned off at the end of the desired period, then wait for the
completion of the desired PRI.

C. FOURIER SYNTHESIS FOR CODED WAVEFORMS

A coded waveform is a pulse sequence which contains N subpulses of equal duration. The subpulses of opposite polarity are arranged in a certain sequence to achieve a spiky autocorrelation with minimum sidelobes.

1. Reasons for Coded Waveforms

In conventional radars, the pulse compression scheme allows a radar to utilize a long coded pulse to achieve higher radiated energy for longer detection ranges, while it still retains the range resolution of short pulses. The same idea can be used in UWB radars. The purpose of this is to put more energy on the target. The coded pulses can be generated by the Fourier method, as described in the next section.

2. Mathematics for Generation of Coded Waveforms

A Fourier series expansion for the function $x(t)$ can be determined more easily by differentiating the function, if the resulting expression is of the form of a delta function sequence. Differentiation of rectangular pulses indeed results in delta function sequences. A delta function sequences can be expressed as the sum of the cosine waveforms, which makes it possible to determine the Fourier series coefficients.

From equation (4.5), the approximate Fourier series expansion is

$$x(t) \approx \sum_{n=1}^{N} \left[a_n \cdot \cos\left(\frac{2\pi nt}{T}\right) + b_n \cdot \sin\left(\frac{2\pi nt}{T}\right) \right] . \qquad (4.5)$$

Differentiating both sides with respect to t,

$$x'(t) = \sum_{n=1}^{N} \left[\frac{2\pi n}{T} a_n \cdot \sin\left(\frac{2\pi nt}{T}\right) + \frac{2\pi n}{T} b_n \cdot \cos\left(\frac{2\pi nt}{T}\right) \right] . \qquad (4.14)$$

Let

$$x'(t) = \sum_{n=1}^{N} \left[\alpha_n \cdot \cos\left(\frac{2\pi nt}{T}\right) + \beta_n \cdot \sin\left(\frac{2\pi nt}{T}\right) \right] . \qquad (4.15)$$

where

$$\alpha_n = \frac{2\pi n}{T} \cdot b_n , \qquad \beta_n = \frac{-2\pi n}{T} \cdot a_n . \qquad (4.16)$$

If $x'(t)$ can be expressed as a delta function sequence, then α_n and β_n can be easily determined by comparing the two sides. Coefficients a_n, b_n are computed from α_n and β_n as follows

$$a_n = -\frac{T}{2\pi n} \cdot \beta_n = -\frac{1}{n w_0} \cdot \beta_n ,$$

$$b_n = \frac{T}{2\pi n} \cdot \alpha_n = \frac{1}{n w_0} \cdot \alpha_n . \qquad (4.17)$$

3. Examples

In conventional radars, pulse compression waveforms are generated by phase coding sinusoidal signals (i.e., 0" phase shift for '+', and 180" phase shift for '-'). Binary coded waveforms for UWB radars can be generated by using the

31

polarity of the pulse (i.e., positive amplitude for '+' and negative amplitude for '-'). Any binary coded sequence can be approximated using the Fourier series. In the following examples a Barker code sequence of length 5 will be considered; this sequence is "+ + + - +".

a. Continuous Wave Coded Waveforms

In continuous wave coded waveforms, the ratio of the number of subpulses per PRI to the code word length is one (i.e., the code waveform will repeat itself continuously). Using polar signaling as the coded format, a Barker code of length 5 is shown in Figure (4.7a) where "+" is represented with a rectangular pulse of amplitude A and "-" is represented by a rectangular pulse of amplitude -A. Thus, a long coded pulse of duration T consists of five subpulses each of length T/5. This continuous wave coded waveform can be mathematically represented as

$$x(t) = A \sum_{n=-\infty}^{\infty} \prod(t - nT) + A \cdot \sum_{n=-\infty}^{\infty} \prod(t - nT - \frac{T}{5}) + A \cdot \sum_{n=-\infty}^{\infty} \prod(t - nT - \frac{2T}{5})$$

$$- A \cdot \sum_{n=-\infty}^{\infty} \prod(t - nT - \frac{3T}{5}) + A \cdot \sum_{n=-\infty}^{\infty} \prod(t - nT - \frac{4T}{5}) ,$$

$$(4.18)$$

where

$$\prod(t) = \begin{cases} 1, & 0 < t < \frac{T}{5} ; \\ 0, & \frac{T}{5} < t < T . \end{cases}$$

Differentiating both sides of equation (4.18),

$$x'(t) = A \cdot \left[\sum_{n=-\infty}^{\infty} \delta(t-nT) - \sum_{n=-\infty}^{\infty} \delta(t-nT-\frac{T}{5}) \right]$$

$$+ A \cdot \left[\sum_{n=-\infty}^{\infty} \delta(t-nT-\frac{T}{5}) - \sum_{n=-\infty}^{\infty} \delta(t-nT-\frac{2T}{5}) \right]$$

$$+ A \cdot \left[\sum_{n=-\infty}^{\infty} \delta(t-nT-\frac{2T}{5}) - \sum_{n=-\infty}^{\infty} \delta(t-nT-\frac{3T}{5}) \right] \quad (4.19)$$

$$- A \cdot \left[\sum_{n=-\infty}^{\infty} \delta(t-nT-\frac{3T}{5}) - \sum_{n=-\infty}^{\infty} \delta(t-nT-\frac{4T}{5}) \right]$$

$$+ A \cdot \left[\sum_{n=-\infty}^{\infty} \delta(t-nT-\frac{4T}{5}) - \sum_{n=-\infty}^{\infty} \delta(t-nT-\frac{5T}{5}) \right] .$$

Regrouping terms in equation (4.19),

$$x'(t) = A \cdot \sum_{n=-\infty}^{\infty} \delta(t-nT) - 2A \cdot \sum_{n=-\infty}^{\infty} \delta\left(t-nT-\frac{3T}{5}\right)$$

$$\quad (4.20)$$

$$+ 2A \cdot \sum_{n=-\infty}^{\infty} \delta\left(t-nT-\frac{4T}{5}\right) - A \cdot \sum_{n=-\infty}^{\infty} \delta\left(t-nT-\frac{5T}{5}\right) .$$

Equation (4.20) can be plotted as Figure (4.7b).

Delta function sequence $\delta_T(t)$ can be represented as

$$\delta_T(t) = \sum_{n=-\infty}^{\infty} \delta(t-nT) = \frac{1}{T} + \frac{2}{T} \cdot \sum_{n=1}^{\infty} \cos(nw_0 t) . \quad (4.21)$$

Derivation of the above equation is given in Appendix A.
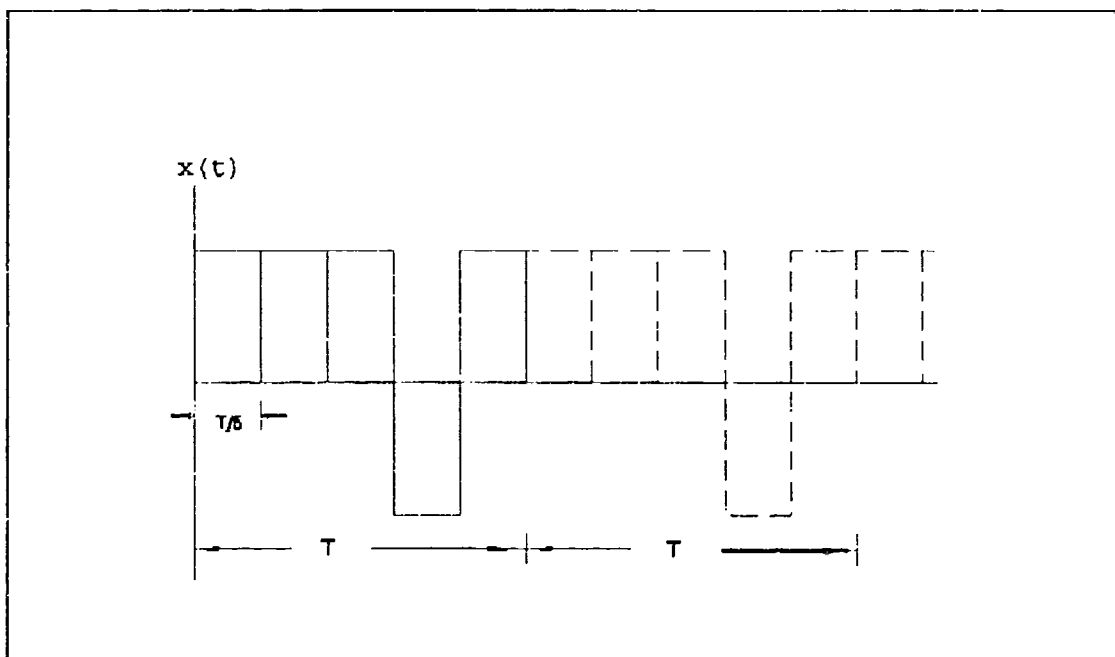
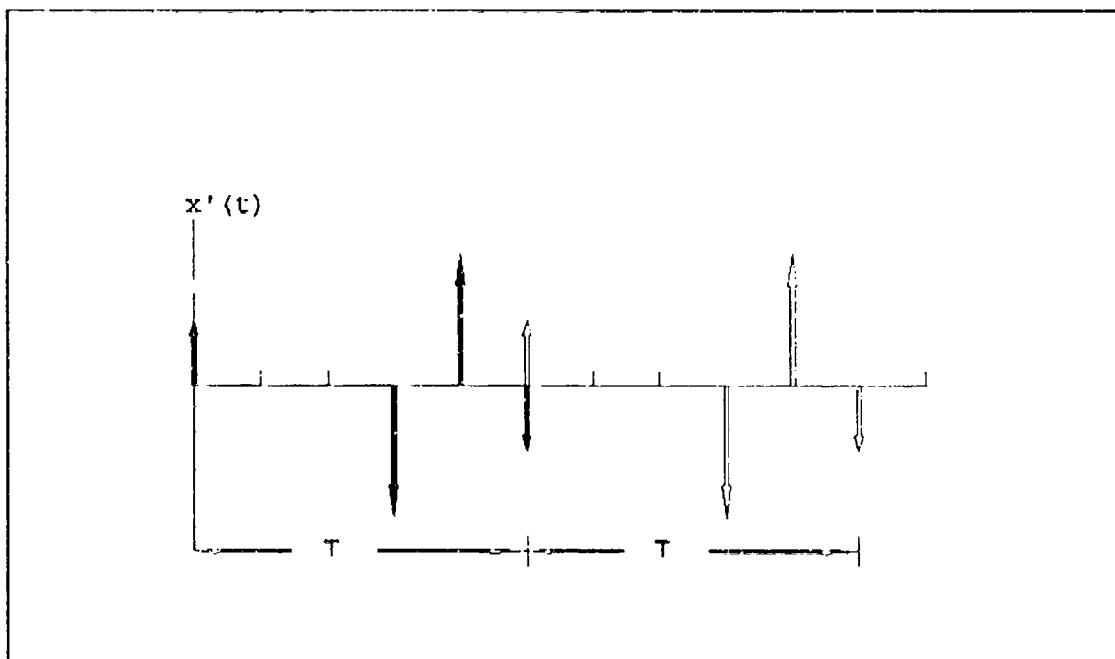Figure 4.7a   Coded rectangular pulse train
(code + + + - +).

Figure 4.7b   Delta function sequence,
derivative of Figure 4.7a.

34

From equation (4.20) and (4.21),

$$x'(t) = A \cdot \left[\frac{1}{T} + \frac{2}{T} \cdot \sum_{n=1}^{\infty} \cos(nw_0 t) \right] - 2A \cdot \left[\frac{1}{T} + \frac{2}{T} \cdot \sum_{n=1}^{\infty} \cos\left(nw_0\left(t - \frac{3T}{5}\right)\right) \right]$$

$$+ 2A \cdot \left[\frac{1}{T} + \frac{2}{T} \cdot \sum_{n=1}^{\infty} \cos\left(nw_0\left(t - \frac{4T}{5}\right)\right) \right] - A \cdot \left[\frac{1}{T} + \frac{2}{T} \cdot \sum_{n=1}^{\infty} \cos\left(nw_0\left(t - \frac{5T}{5}\right)\right) \right]$$

$$(4.22)$$

All 1/T terms are canceled, and equation (4.22) reduces to

$$x'(t) = \frac{2A}{T} \cdot \sum_{n=1}^{\infty} \cos(nw_0 t) - \frac{4A}{T} \cdot \sum_{n=1}^{\infty} \cos\left[nw_0\left(t - \frac{3T}{5}\right)\right]$$

$$+ \frac{4A}{T} \cdot \sum_{n=1}^{\infty} \cos\left[nw_0\left(t - \frac{4T}{4}\right)\right] - \frac{2A}{T} \cdot \sum_{n=1}^{\infty} \cos\left[nw_0\left(t - \frac{5T}{5}\right)\right] \ .$$

$$(4.23)$$

Applying the trigonometric compound formula, the equation can be expanded to

$$x'(t) = \frac{2A}{T} \cdot \sum_{n=1}^{\infty} \cos(nw_0 t)$$

$$- \frac{2A}{T} \cdot \sum_{n=1}^{\infty} 2 \cdot \left[\cos(nw_0 t) \cdot \cos\left(n \cdot \frac{2\pi}{T} \cdot \frac{3T}{5}\right) + \sin(nw_0 t) \cdot \sin\left(n \cdot \frac{2\pi}{T} \cdot \frac{3T}{5}\right) \right]$$

$$+ \frac{2A}{T} \cdot \sum_{n=1}^{\infty} 2 \cdot \left[\cos(nw_0 t) \cdot \cos\left(n \cdot \frac{2\pi}{T} \cdot \frac{4T}{5}\right) + \sin(nw_0 t) \cdot \sin\left(n \cdot \frac{2\pi}{T} \cdot \frac{4T}{5}\right) \right]$$

$$- \frac{2A}{T} \cdot \sum_{n=1}^{\infty} \left[\cos(nw_0 t) \cdot \cos\left(n \cdot \frac{2\pi}{T} \cdot \frac{5T}{5}\right) + \sin(nw_0 t) \cdot \sin\left(n \cdot \frac{2\pi}{T} \cdot \frac{5T}{5}\right) \right] \ .$$

$$(4.24)$$

Regrouping terms in equation (4.24), one gets

35

$$x'(t) = \frac{2A}{T} \cdot \sum_{n=1}^{\infty} \cos(nw_0 t) \cdot \left(1 - 2\cos\frac{6n\pi}{5} + 2\cos\frac{8n\pi}{5} - \cos\frac{10n\pi}{5} \right)$$

$$- \frac{2A}{T} \cdot \sum_{n=1}^{\infty} \sin(nw_0 t) \cdot \left(2\sin\frac{6n\pi}{5} - 2\sin\frac{8n\pi}{5} + 2\sin\frac{10n\pi}{5} \right) .$$

$$(4.25)$$

The coefficient of the $\cos(nw_0 t)$ term has been defined as α_n, and the coefficient of the $\sin(nw_0 t)$ term has been defined as β_n in equation (4.15). Thus, from equation (4.25):

$$\alpha_n = \frac{2A}{T} \cdot \left[1 - 2\cos\frac{6n\pi}{5} + 2\cos\frac{8n\pi}{5} - \cos\frac{10n\pi}{5} \right] , \quad (4.26)$$

$$\beta_n = -\frac{2A}{T} \cdot \left[2\sin\frac{6n\pi}{5} - 2\sin\frac{8n\pi}{5} + \sin\frac{10n\pi}{5} \right] . \quad (4.27)$$

Substituting expressions for α_n and β_n in equations (4.26) and (4.27) into equation (4.17), Fourier coefficients a_n and b_n are:

$$a_n = \frac{A}{n\pi} \cdot \left(2\sin\frac{6n\pi}{5} - 2\sin\frac{8n\pi}{5} + \sin\frac{10n\pi}{5} \right) , \quad (4.28)$$

$$b_n = \frac{A}{n\pi} \cdot \left(1 - 2\cos\frac{6n\pi}{5} + 2\cos\frac{8n\pi}{5} - \cos\frac{10n\pi}{5} \right) . \quad (4.29)$$

Substituting coefficients a_n and b_n into equation (4.5), one obtains the Fourier series expansion for the continuous wave coded waveform:

$$x(t) = \frac{A}{n\pi} \cdot \sum_{n=1}^{N} \left\{ \left[2\sin\frac{6n\pi}{5} - 2\sin\frac{8n\pi}{5} + \sin\frac{10n\pi}{5} \right] \cdot \cos(nw_0 t) \right\}$$

$$+ \frac{A}{n\pi} \cdot \sum_{n=1}^{N} \left\{ \left[1 - 2\cos\frac{6n\pi}{5} + 2\cos\frac{8n\pi}{5} - \cos\frac{10n\pi}{5} \right] \cdot \sin(nw_0 t) \right\}$$

$$(4.30)$$

Figure (4.8) shows that the continuous wave coded waveform for a unit amplitude and fundamental frequency f_0 is equal to 0.25 GHz. The number of harmonics used is nine in Figure (4.8a) and 64 in Figure (4.8b). Using the same approach, other coded waveforms can be derived.
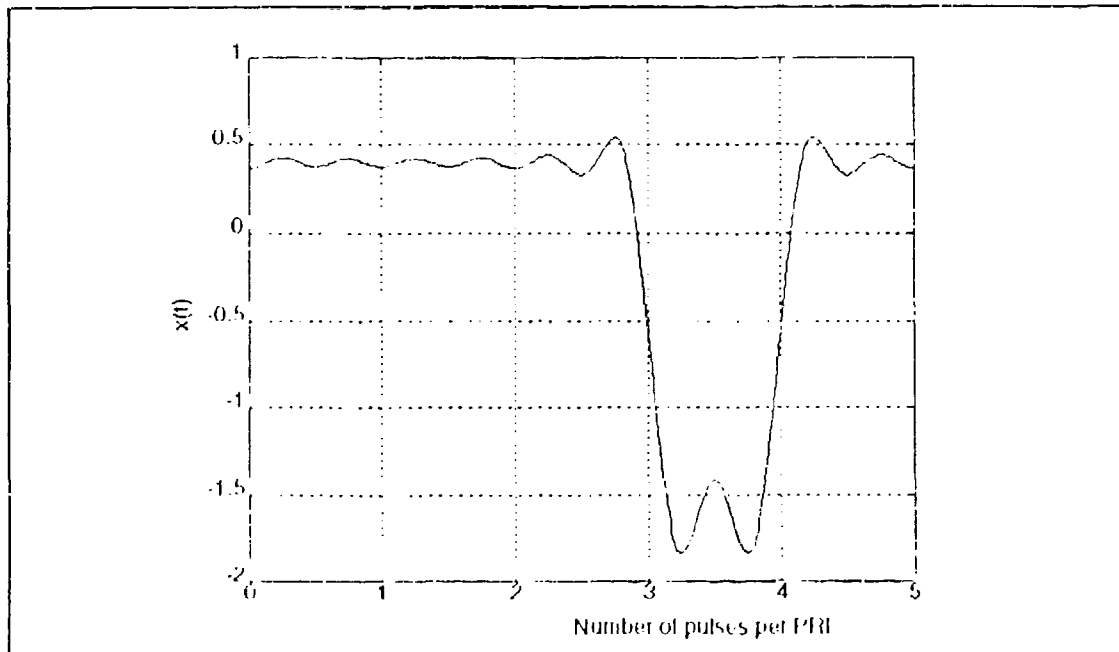
Figure 4.8a   Continuous wave coded waveform (code + + + -
               +), and PRF=0.25 GHz, ratio=1, N=9.
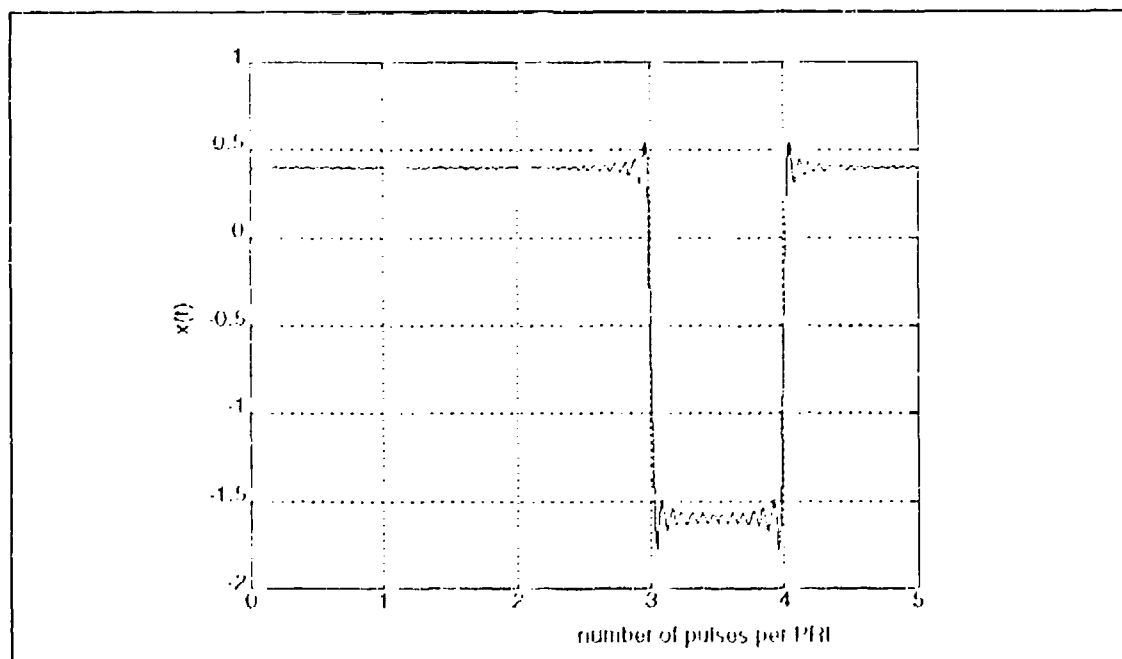
Figure 4.8b   Continuous wave coded waveform (code + + + -
               +), and PRF=0.25 GHz, ratio=1, N=64.

b.   *Pulsed Coded Waveforms*

Unlike the previous case, in this section the coded waveform does not repeat continuously without a pause. A pause period follows the coded waveform. This pattern of a coded waveform followed by a pause, forms the coded pulse train. Figure (4.9a) shows a coded waveform with the ratio of the number of subpulses per PRI to the code word length equal to 2 which means a long coded pulse of duration T consisting of 10 subpulses in sequence (i.e., + + + - + 0 0 0 0 0) each of length T/10. For this waveform, the Barker code of length 5 can be mathematically represented as:

$$x(t) = A \cdot \sum_{n=-\infty}^{\infty} \Pi(t - nT) + A \cdot \sum_{n=-\infty}^{\infty} \Pi(t - nT - \frac{T}{10}) + A \cdot \sum_{n=-\infty}^{\infty} \Pi(t - nT - \frac{2T}{10})$$

$$- A \cdot \sum_{n=-\infty}^{\infty} \Pi(t - nT - \frac{3T}{10}) + A \cdot \sum_{n=-\infty}^{\infty} \Pi(t - nT - \frac{4T}{10}) ,$$

$$(4.31)$$

where

$$\Pi(t) = \begin{cases} 1, & 0 < t < \frac{T}{10} ; \\ 0, & \frac{T}{10} < t < T . \end{cases}$$

Differentiating both sides of equation (4.31), one gets

$$x'(t) = A \cdot \left[\sum_{n=-\infty}^{\infty} \delta(t-nT) - \sum_{n=-\infty}^{\infty} \delta(t-nT-\frac{T}{10}) \right]$$

$$+ A \cdot \left[\sum_{n=-\infty}^{\infty} \delta(t-nT-\frac{T}{10}) - \sum_{n=-\infty}^{\infty} \delta(t-nT-\frac{2T}{10}) \right]$$

$$+ A \cdot \left[\sum_{n=-\infty}^{\infty} \delta(t-nT-\frac{2T}{10}) - \sum_{n=-\infty}^{\infty} \delta(t-nT-\frac{3T}{10}) \right] \qquad (4.32)$$

$$- A \cdot \left[\sum_{n=-\infty}^{\infty} \delta(t-nT-\frac{3T}{10}) - \sum_{n=-\infty}^{\infty} \delta(t-nT-\frac{4T}{10}) \right]$$

$$+ A \cdot \left[\sum_{n=-\infty}^{\infty} \delta(t-nT-\frac{4T}{10}) - \sum_{n=-\infty}^{\infty} \delta(t-nT-\frac{5T}{10}) \right] .$$

Regrouping equation (4.32),

$$x'(t) = A \cdot \sum_{n=-\infty}^{\infty} \delta(t-nT) - 2A \cdot \sum_{n=-\infty}^{\infty} \delta\left(t-nT-\frac{3T}{10}\right)$$

$$+ 2A \cdot \sum_{n=-\infty}^{\infty} \delta\left(t-nT-\frac{4T}{10}\right) - A \cdot \sum_{n=-\infty}^{\infty} \delta\left(t-nT-\frac{5T}{10}\right) . \qquad (4.33)$$

Equation (4.33) can be plotted as Figure (4.9b). From equations (4.21) and (4.33),

$$x'(t) = A \cdot \left[\frac{1}{T} + \frac{2}{T} \cdot \sum_{n=1}^{\infty} \cos(nw_0 t) \right] - 2A \cdot \left[\frac{1}{T} + \frac{2}{T} \cdot \sum_{n=1}^{\infty} \cos\left(nw_0\left(t-\frac{3T}{10}\right)\right) \right]$$

$$+ 2A \cdot \left[\frac{1}{T} + \frac{2}{T} \cdot \sum_{n=1}^{\infty} \cos\left(nw_0\left(t-\frac{4T}{10}\right)\right) \right] - A \cdot \left[\frac{1}{T} + \frac{2}{T} \cdot \sum_{n=1}^{\infty} \cos\left(nw_0\left(t-\frac{5T}{10}\right)\right) \right] .$$
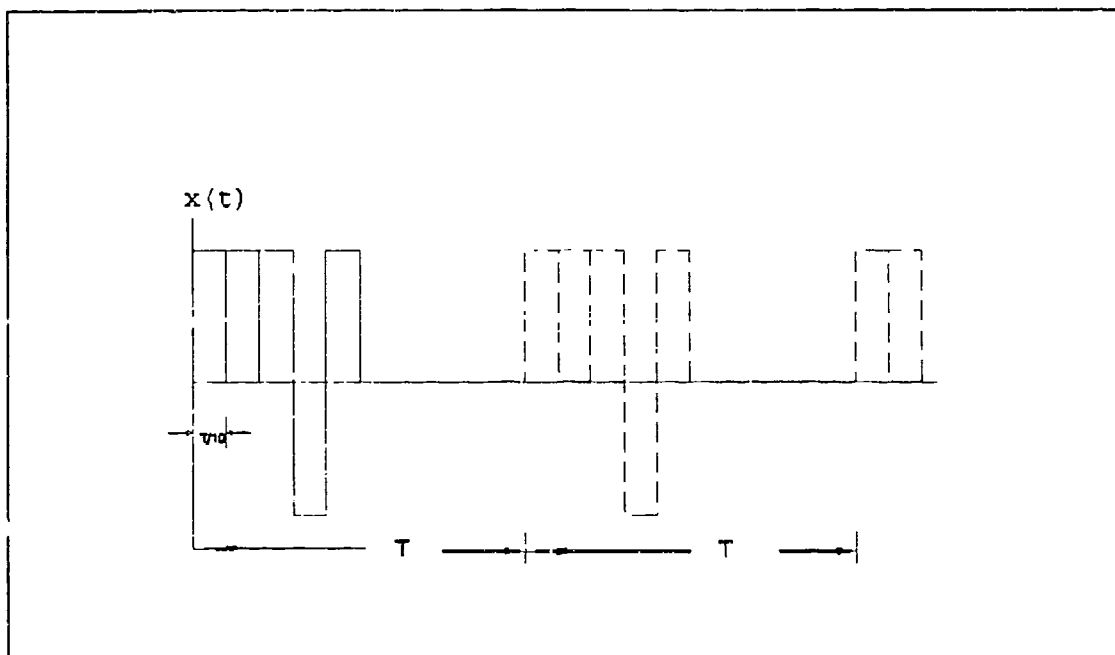
$$(4.34)$$

Figure 4.9a   Coded rectangular pulse train
(code + + + - + 0 0 0 0 0).
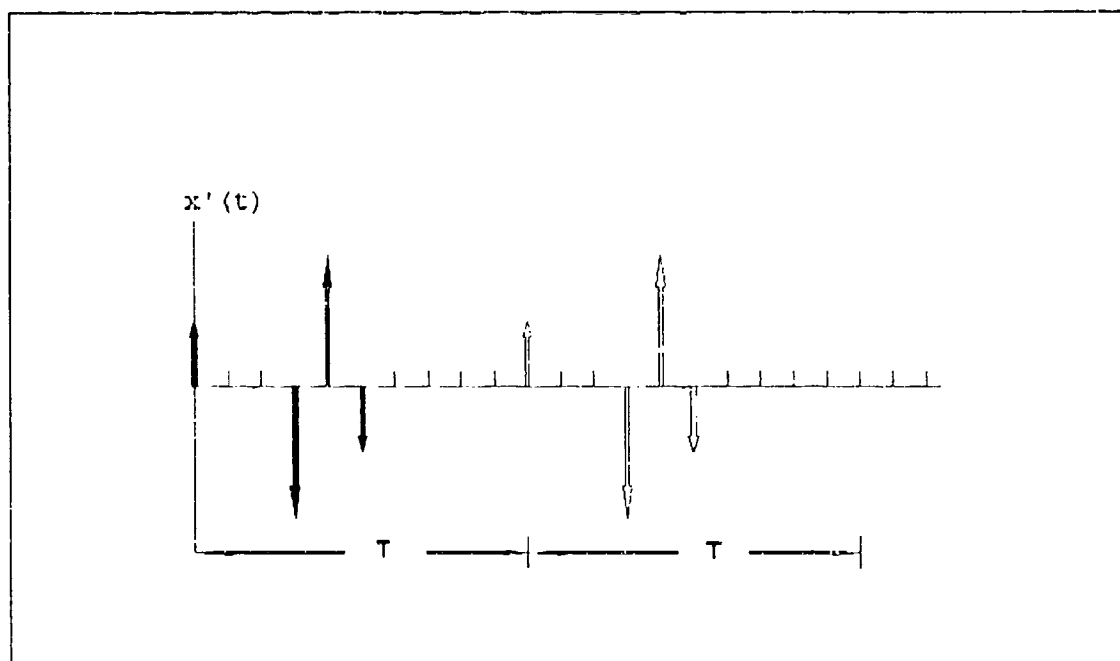

Figure 4.9b   Delta function sequence,
derivative of Figure 4.9a.

41

All 1/T terms are canceled, and equation (4.34) reduces to

$$x'(t) = \frac{2A}{T} \cdot \sum_{n=1}^{\infty} \cos(nw_0 t) - \frac{4A}{T} \cdot \sum_{n=1}^{\infty} \cos\left[nw_0\left(t - \frac{3T}{10}\right)\right]$$
$$+ \frac{4A}{T} \cdot \sum_{n=1}^{\infty} \cos\left[nw_0\left(t - \frac{4T}{10}\right)\right] - \frac{2A}{T} \cdot \sum_{n=1}^{\infty} \cos\left[nw_0\left(t - \frac{5T}{10}\right)\right].$$

(4.35)

Applying the trigonometric compound formula, the equation (4.35) can be expanded to

$$x'(t) = \frac{2A}{T} \cdot \sum_{n=1}^{\infty} \cos(nw_0 t)$$

$$- \frac{2A}{T} \cdot \sum_{n=1}^{\infty} 2 \cdot \left[\cos(nw_0 t) \cdot \cos\left(n \cdot \frac{2\pi}{T} \cdot \frac{3T}{10}\right) + \sin(nw_0 t) \cdot \sin\left(n \cdot \frac{2\pi}{T} \cdot \frac{3T}{10}\right)\right]$$

$$+ \frac{2A}{T} \cdot \sum_{n=1}^{\infty} 2 \cdot \left[\cos(nw_0 t) \cdot \cos\left(n \cdot \frac{2\pi}{T} \cdot \frac{4T}{10}\right) + \sin(nw_0 t) \cdot \sin\left(n \cdot \frac{2\pi}{T} \cdot \frac{4T}{10}\right)\right]$$

$$- \frac{2A}{T} \cdot \sum_{n=1}^{\infty} \left[\cos(nw_0 t) \cdot \cos\left(n \cdot \frac{2\pi}{T} \cdot \frac{5T}{10}\right) + \sin(nw_0 t) \cdot \sin\left(n \cdot \frac{2\pi}{T} \cdot \frac{5T}{10}\right)\right].$$

(4.36)

Regrouping terms in equation (4.36), one gets

$$x'(t) = \frac{2A}{T} \cdot \sum_{n=1}^{\infty} \cos(nw_0 t) \cdot \left(1 - 2\cos\frac{6n\pi}{10} + 2\cos\frac{8n\pi}{10} - \cos\frac{10n\pi}{10}\right)$$

$$- \frac{2A}{T} \cdot \sum_{n=1}^{\infty} \sin(nw_0 t) \cdot \left(2\sin\frac{6n\pi}{10} - 2\sin\frac{8n\pi}{10} + 2\sin\frac{10n\pi}{10}\right).$$

(4.37)

Using equations (4.15) and (4.37), α_n and β_n can be determined as

$$\alpha_n = \frac{2A}{T} \cdot \left[1 - 2\cos\frac{6n\pi}{10} + 2\cos\frac{8n\pi}{10} - \cos\frac{10n\pi}{10}\right], \quad (4.38)$$

42

$$\beta_n = -\frac{2A}{T} \cdot \left[2\sin\frac{6n\pi}{10} - 2\sin\frac{8n\pi}{10} + \sin\frac{10n\pi}{10} \right] . \quad (4.39)$$

Substituting expressions for α_n and β_n from equations (4.38) and (4.39) into equation (4.17), Fourier coefficients a_n and b_n can be obtained as

$$a_n = \frac{A}{n\pi} \cdot \left(2\sin\frac{6n\pi}{10} - 2\sin\frac{8n\pi}{10} + \sin\frac{10n\pi}{10} \right) , \quad (4.40)$$

$$b_n = \frac{A}{n\pi} \cdot \left(1 - 2\cos\frac{6n\pi}{10} + 2\cos\frac{8n\pi}{10} - \cos\frac{10n\pi}{10} \right) . \quad (4.41)$$

Substituting coefficients a_n and b_n into equation (4.5), one gets the Fourier series expansion for the pulsed coded waveform:

$$x(t) = \frac{A}{n\pi} \cdot \sum_{n=1}^{N} \left\{ \left[2\sin\frac{6n\pi}{10} - 2\sin\frac{8n\pi}{10} + \sin\frac{10n\pi}{10} \right] \cdot \cos(nw_0 t) \right\}$$

$$+ \frac{A}{n\pi} \cdot \sum_{n=1}^{N} \left\{ \left[1 - 2\cos\frac{6n\pi}{10} + 2\cos\frac{8n\pi}{10} - \cos\frac{10n\pi}{10} \right] \cdot \sin(nw_0 t) \right\} .$$

$$(4.42)$$

It should be noted that in this case no switching is required to generate a pause period.

Figure (4.10) shows a coded waveform for a fundamental frequency f_0 of 0.25 GHz. The number of harmonics used are nine in Figure (4.10a) and 64 in Figure (4.10b).
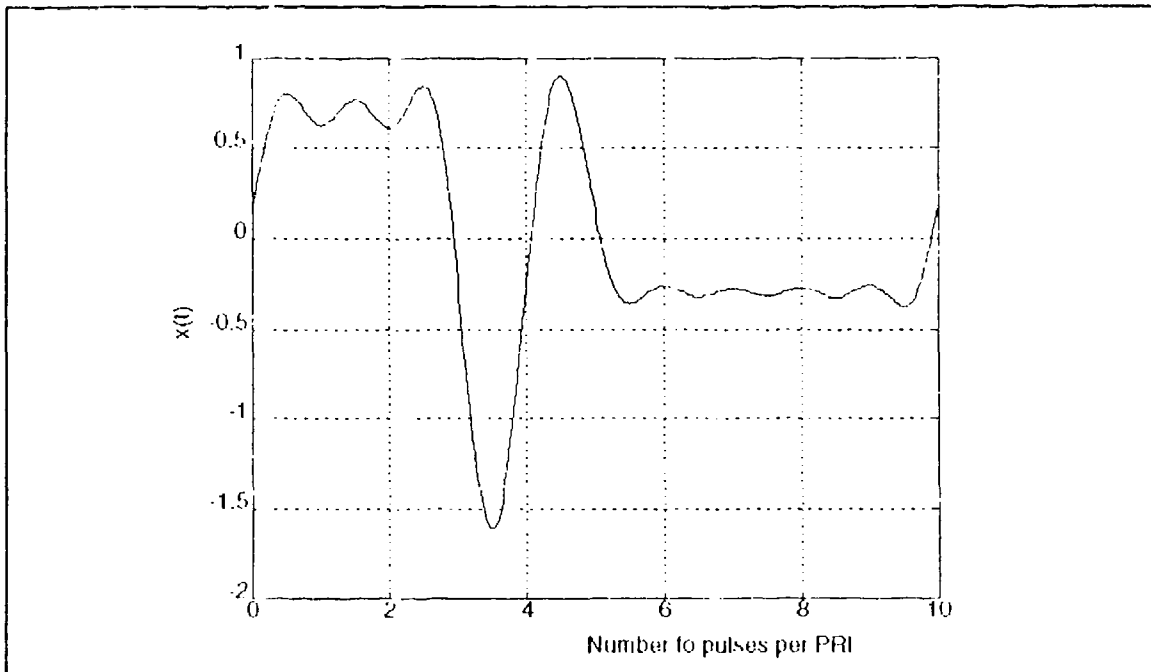
Figure 4.10a   Pulsed coded waveform (code + + + - +), and
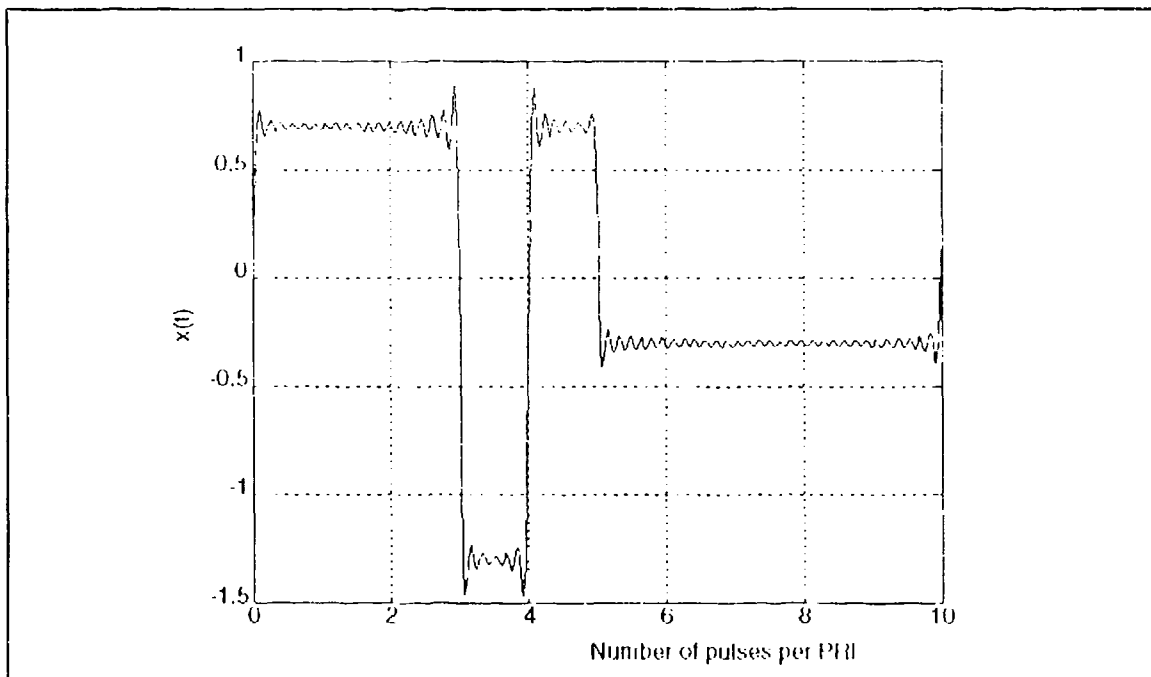   PRF=0.25 GHz, ratio=2, N=9.

Figure 4.10b   Pulsed coded waveform (code + + + - +), and
                PRF=0.25 GHz, ratio=2, N=64.

44

Practical coded radar signals can be generated with or without switching. Switching is used if a signal with a long PRI is required. Oscillators can be turned on at the beginning of the coded sequence and turned off at the completion of the sequence. Although a switch is used, it is still better than having to switch after every subpulse in the sequence. However, if a coded radar signal with a relatively high PRF is required, no switching is needed at all to generate the coded pulses. This is an advantage, since fast switching is one of the technical hurdles in ultra-wideband radar technology.

c. Other Coded Waveforms

This technique of Fourier expansion is also valid for other kinds of codes as long as after successive differentiations, the resulting expression only consists of delta functions.

The following example shows a basic subpulse consisting of a half rectangular pulse and a half zero pulse. Assuming that the ratio of the number of subpulses per PRI to the code word length is one, then the coded waveform will repeat itself without any pause period. The "+" is represented by the half pulse of amplitude A, the other half pulse of zero and the "-" is represented by the half pulse of amplitude -A, the other half pulse of zero. Barker code of length 5, as shown in Figure (4.11a) can be mathematically represented as

$$x(t) = A \cdot \sum_{n=-\infty}^{\infty} \prod(t-nT) + A \cdot \sum_{n=-\infty}^{\infty} \prod(t-nT-\frac{2T}{10})$$

$$+ A \cdot \sum_{n=-\infty}^{\infty} \prod(t-nT-\frac{4T}{10}) - A \cdot \sum_{n=-\infty}^{\infty} \prod(t-nT-\frac{6T}{10}) \qquad (4.43)$$

$$+ A \cdot \sum_{n=-\infty}^{\infty} \prod(t-nT-\frac{8T}{10}) ,$$

where

$$\prod(t) = \begin{cases} 1, & 0 < t < \frac{T}{10} \ ; \\ 0, & \frac{T}{10} < t < T \ . \end{cases}$$

For computation purposes, the time axis in x(t) is shifted. Shifted x(t) can be written as

$$x(t) = A \cdot \sum_{n=-\infty}^{\infty} \prod(t-nT) + A \cdot \sum_{n=-\infty}^{\infty} \prod(t-nT-\frac{2T}{10})$$

$$+ A \cdot \sum_{n=-\infty}^{\infty} \prod(t-nT-\frac{4T}{10}) - A \cdot \sum_{n=-\infty}^{\infty} \prod(t-nT+\frac{4T}{10}) \qquad (4.44)$$

$$+ A \cdot \sum_{n=-\infty}^{\infty} \prod(t-nT+\frac{2T}{10}) .$$

Differentiating both sides of equation (4.44),

$$x'(t) = \left[A \cdot \sum_{n=-\infty}^{\infty} \delta(t - nT) - A \cdot \sum_{n=-\infty}^{\infty} \delta\left(t - nT - \frac{T}{10}\right) \right]$$

$$+ \left[A \cdot \sum_{n=-\infty}^{\infty} \delta\left(t - nT - \frac{2T}{10}\right) - A \cdot \sum_{n=-\infty}^{\infty} \delta\left(t - nT - \frac{3T}{10}\right) \right]$$

$$+ \left[A \cdot \sum_{n=-\infty}^{\infty} \delta\left(t - nT - \frac{4T}{10}\right) - A \cdot \sum_{n=-\infty}^{\infty} \delta\left(t - nT - \frac{5T}{10}\right) \right] \qquad (4.45)$$

$$- \left[A \cdot \sum_{n=-\infty}^{\infty} \delta\left(t - nT + \frac{4T}{10}\right) - A \cdot \sum_{n=-\infty}^{\infty} \delta\left(t - nT + \frac{3T}{10}\right) \right]$$

$$+ \left[A \cdot \sum_{n=-\infty}^{\infty} \delta\left(t - nT + \frac{2T}{10}\right) - A \cdot \sum_{n=-\infty}^{\infty} \delta\left(t - nT + \frac{T}{10}\right) \right].$$

The resulting function is shown in Figure (4.11b). Substituting the expression for $\delta_T(t)$ from equation (4.21) in equation (4.45), gives

$$x'(t) = \frac{2A}{T} \cdot \sum_{n=1}^{\infty} \cos(nw_0 t) - \frac{2A}{T} \cdot \sum_{n=1}^{\infty} \cos\left[nw_0\left(t - \frac{T}{10}\right)\right]$$

$$+ \frac{2A}{T} \cdot \sum_{n=1}^{\infty} \cos\left[nw_0\left(t - \frac{2T}{10}\right)\right] - \frac{2A}{T} \cdot \sum_{n=1}^{\infty} \cos\left[nw_0\left(t - \frac{3T}{10}\right)\right]$$

$$+ \frac{2A}{T} \cdot \sum_{n=1}^{\infty} \cos\left[nw_0\left(t - \frac{4T}{10}\right)\right] - \frac{2A}{T} \cdot \sum_{n=1}^{\infty} \cos\left[nw_0\left(t - \frac{5T}{10}\right)\right] \qquad (4.46)$$

$$- \frac{2A}{T} \cdot \sum_{n=1}^{\infty} \cos\left[nw_0\left(t + \frac{4T}{10}\right)\right] + \frac{2A}{T} \cdot \sum_{n=1}^{\infty} \cos\left[nw_0\left(t + \frac{3T}{10}\right)\right]$$

$$+ \frac{2A}{T} \cdot \sum_{n=1}^{\infty} \cos\left[nw_0\left(t + \frac{2T}{10}\right)\right] - \frac{2A}{T} \cdot \sum_{n=1}^{\infty} \cos\left[nw_0\left(t + \frac{T}{10}\right)\right].$$
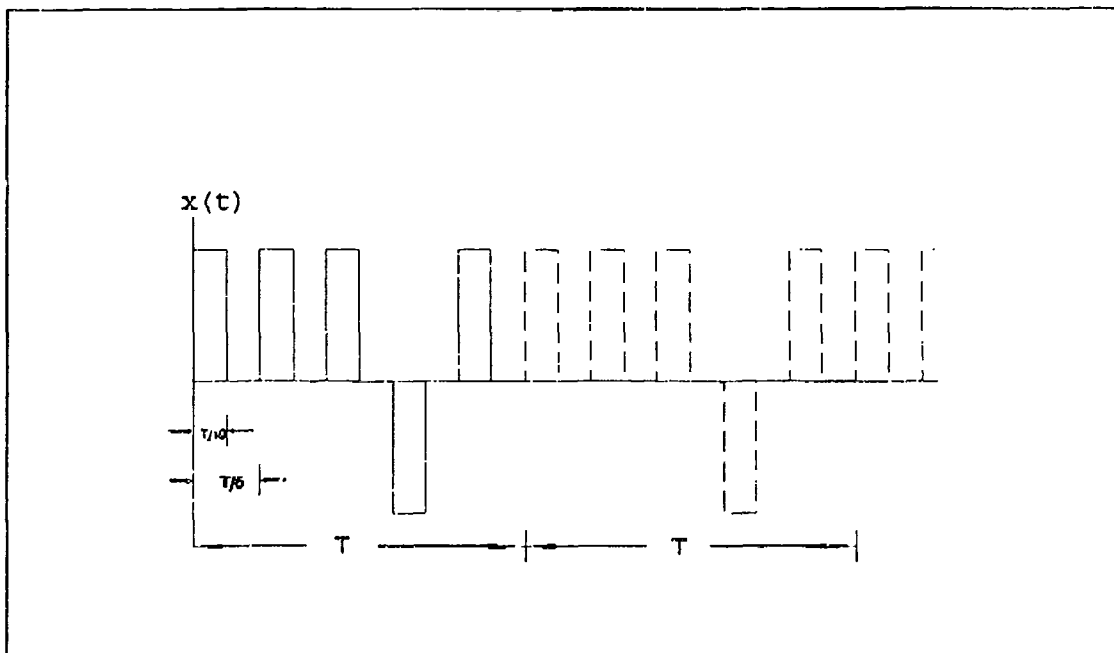
Figure 4.11a   Coded rectangular pulse train
                (special code + + + - +).
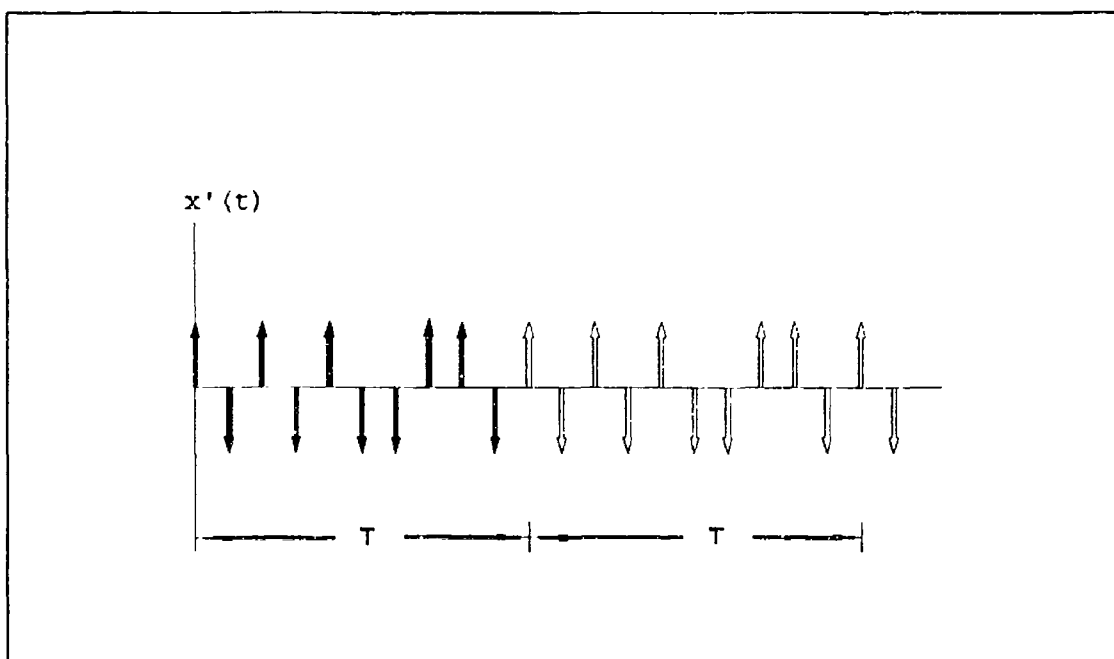

Figure 4.11b   Delta function sequence,
                derivative of Figure 4.11a.

48

Applying the trigonometric compound formula, equation (4.46) can be expanded to

$$
x'(t) = \frac{2A}{T} \cdot \sum_{n=1}^{\infty} \cos(nw_0 t)
$$

$$
- \frac{2A}{T} \cdot \sum_{n=1}^{\infty} \cdot \left[\cos(nw_0 t) \cdot \cos\left(n \cdot \frac{2\pi}{T} \cdot \frac{T}{10}\right) + \sin(nw_0 t) \cdot \sin\left(n \cdot \frac{2\pi}{T} \cdot \frac{T}{10}\right) \right]
$$

$$
+ \frac{2A}{T} \cdot \sum_{n=1}^{\infty} \cdot \left[\cos(nw_0 t) \cdot \cos\left(n \cdot \frac{2\pi}{T} \cdot \frac{2T}{10}\right) + \sin(nw_0 t) \cdot \sin\left(n \cdot \frac{2\pi}{T} \cdot \frac{2T}{10}\right) \right]
$$

$$
- \frac{2A}{T} \cdot \sum_{n=1}^{\infty} \left[\cos(nw_0 t) \cdot \cos\left(n \cdot \frac{2\pi}{T} \cdot \frac{3T}{10}\right) + \sin(nw_0 t) \cdot \sin\left(n \cdot \frac{2\pi}{T} \cdot \frac{3T}{10}\right) \right]
$$

$$
+ \frac{2A}{T} \cdot \sum_{n=1}^{\infty} \cdot \left[\cos(nw_0 t) \cdot \cos\left(n \cdot \frac{2\pi}{T} \cdot \frac{4T}{10}\right) + \sin(nw_0 t) \cdot \sin\left(n \cdot \frac{2\pi}{T} \cdot \frac{4T}{10}\right) \right]
$$

$$
- \frac{2A}{T} \cdot \sum_{n=1}^{\infty} \cdot \left[\cos(nw_0 t) \cdot \cos\left(n \cdot \frac{2\pi}{T} \cdot \frac{5T}{10}\right) + \sin(nw_0 t) \cdot \sin\left(n \cdot \frac{2\pi}{T} \cdot \frac{5T}{10}\right) \right]
$$

$$
- \frac{2A}{T} \cdot \sum_{n=1}^{\infty} \left[\cos(nw_0 t) \cdot \cos\left(n \cdot \frac{2\pi}{T} \cdot \frac{4T}{10}\right) - \sin(nw_0 t) \cdot \sin\left(n \cdot \frac{2\pi}{T} \cdot \frac{4T}{10}\right) \right]
$$

$$
+ \frac{2A}{T} \cdot \sum_{n=1}^{\infty} \cdot \left[\cos(nw_0 t) \cdot \cos\left(n \cdot \frac{2\pi}{T} \cdot \frac{3T}{10}\right) - \sin(nw_0 t) \cdot \sin\left(n \cdot \frac{2\pi}{T} \cdot \frac{3T}{10}\right) \right]
$$

$$
+ \frac{2A}{T} \cdot \sum_{n=1}^{\infty} \cdot \left[\cos(nw_0 t) \cdot \cos\left(n \cdot \frac{2\pi}{T} \cdot \frac{2T}{10}\right) - \sin(nw_0 t) \cdot \sin\left(n \cdot \frac{2\pi}{T} \cdot \frac{2T}{10}\right) \right]
$$

$$
- \frac{2A}{T} \cdot \sum_{n=1}^{\infty} \left[\cos(nw_0 t) \cdot \cos\left(n \cdot \frac{2\pi}{T} \cdot \frac{T}{10}\right) - \sin(nw_0 t) \cdot \sin\left(n \cdot \frac{2\pi}{T} \cdot \frac{T}{10}\right) \right] \cdot
$$

$$
(4.47)
$$

Regrouping terms in equation (4.47), one gets

$$x(t) = \frac{2A}{T} \cdot \sum_{n=1}^{\infty} \cos(nw_0 t) - \frac{4A}{T} \cdot \sum_{n=1}^{\infty} \cos(nw_0 t) \cdot \cos\frac{n\pi}{5}$$

$$+ \frac{4A}{T} \cdot \sum_{n=1}^{\infty} \cos(nw_0 t) \cdot \cos\frac{2n\pi}{5} - \frac{4A}{T} \cdot \sum_{n=1}^{\infty} \sin(nw_0 t) \cdot \sin\frac{3n\pi}{5}$$

$$+ \frac{4A}{T} \cdot \sum_{n=1}^{\infty} \sin(nw_0 t) \cdot \sin\frac{4n\pi}{5} - \frac{4A}{T} \cdot \sum_{n=1}^{\infty} \cos(nw_0 t) \cdot \cos\frac{5n\pi}{5}$$

$$- \frac{2A}{T} \cdot \sum_{n=1}^{\infty} \sin(nw_0 t) \cdot \sin\frac{5n\pi}{5} \ .$$

$$(4.48)$$

Separating $\cos(nw_0 t)$ terms and $\sin(nw_0 t)$ terms,

$$x'(t) = \frac{2A}{T} \cdot \sum_{n=1}^{\infty} \cos(nw_0 t) \cdot \left(1 - 2\cos\frac{n\pi}{5} + 2\cos\frac{2n\pi}{5} - \cos\frac{5n\pi}{5}\right)$$

$$- \frac{2A}{T} \cdot \sum_{n=1}^{\infty} \sin(nw_0 t) \cdot \left(2\sin\frac{3n\pi}{5} - 2\sin\frac{4n\pi}{5} + \sin\frac{5n\pi}{5}\right) \ .$$

$$(4.49)$$

α_n and β_n can be determined as

$$\alpha_n = \frac{2A}{T} \cdot \left[1 - 2\cos\frac{n\pi}{5} + 2\cos\frac{2n\pi}{5} - \cos\frac{5n\pi}{5}\right] , \quad (4.50)$$

$$\beta_n = -\frac{2A}{T} \cdot \left[2\sin\frac{3n\pi}{5} - 2\sin\frac{4n\pi}{5} + \sin\frac{5n\pi}{5}\right] . \quad (4.51)$$

From equations (4.17), (4.50) and (4.51), Fourier coefficients a_n and b_n can be obtained as

$$a_n = \frac{A}{n\pi} \cdot \left(2\sin\frac{3n\pi}{5} - 2\sin\frac{4n\pi}{5} + \sin\frac{5n\pi}{5}\right) , \quad (4.52)$$

$$b_n = \frac{A}{n\pi} \cdot \left(1 - 2\cos\frac{n\pi}{5} + 2\cos\frac{2n\pi}{5} - \cos\frac{5n\pi}{5}\right) , \quad (4.53)$$

Substituting a_n and b_n into equation (4.5), one gets the expression for this special coded waveform. Figure (4.12) shows this waveform for fundamental frequency of 0.25 GHz. The number of harmonics used in Figure (4.12a) is _ne and in Figure (4.12b) it is 64.

D. Tradeoffs in Coded Waveform Generation

There are tradeoffs involved in the implementation of coded waveforms. The waveform shown in Figure (4.8) is not realistic for practical applications since the positive amplitude is much smaller than the negative amplitude. Figures (4.13a) to (4.13f) show the Barker codes of lengths 3, 4, 5, 7, 11 and 13. From these figures, one can notice that the 7-bit and 11-bit code lengths have more even balances of positive and negative units and therefore would be used more likely. The number of positive going bits should be nearly equal to the number of negative going bits to have a useful sequence.
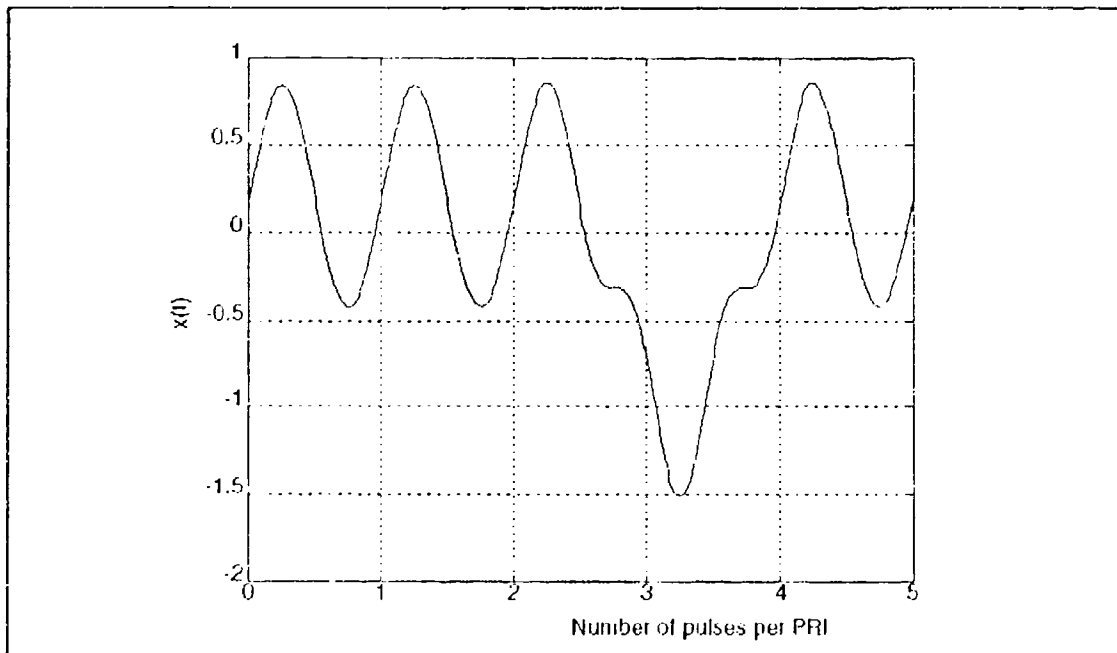
51

Figure 4.12a   Special coded waveform (code + + + - +), and
               PRF=0.25 GHz, ratio=1, N=9.
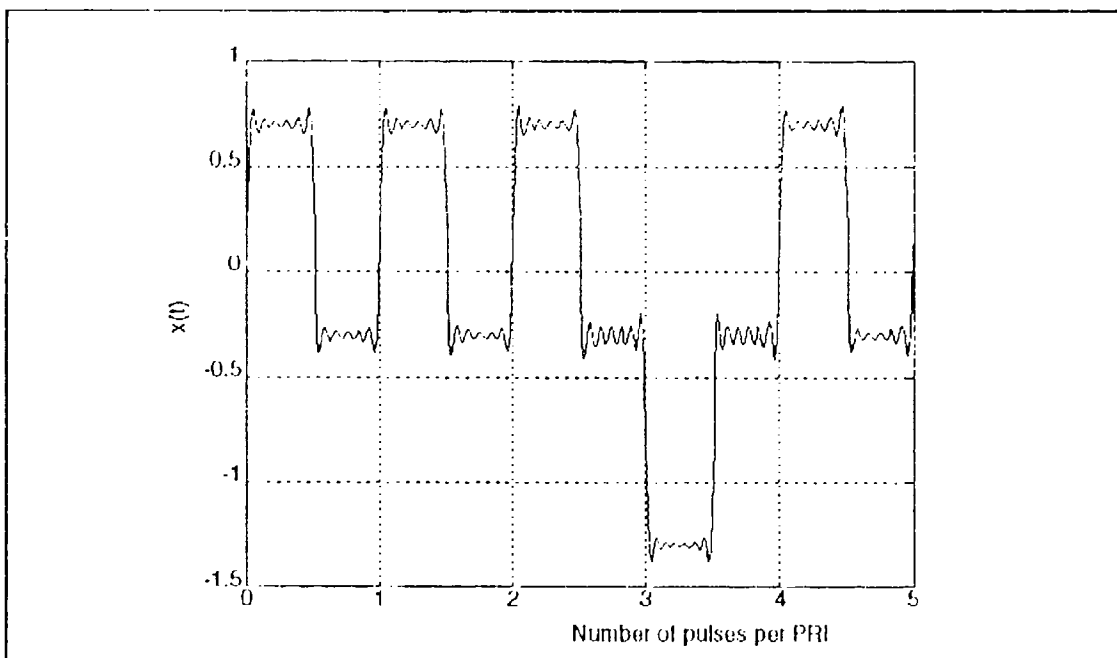

Figure 4.12b   Special coded waveform (code + + + - +), and
               PRF=0.25 GHz, ratio=1, N=64.
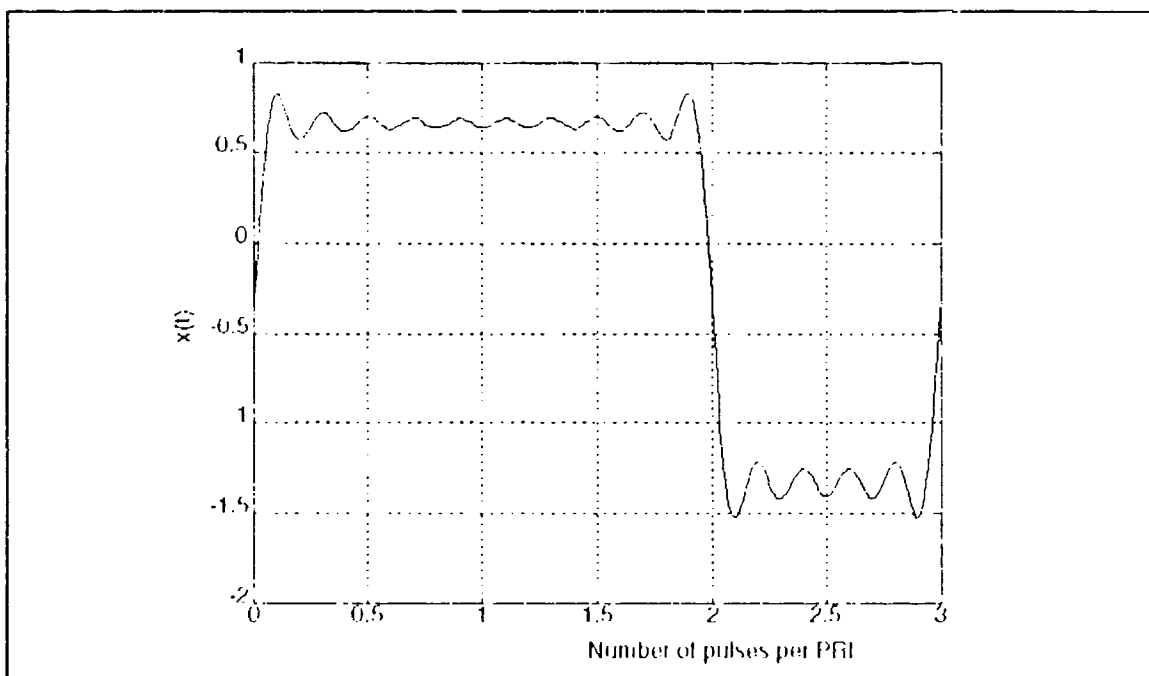
Figure 4.13a   CW coded waveform (code + + -), and
                PRF=0.25 GHz, ratio=1, N=15.

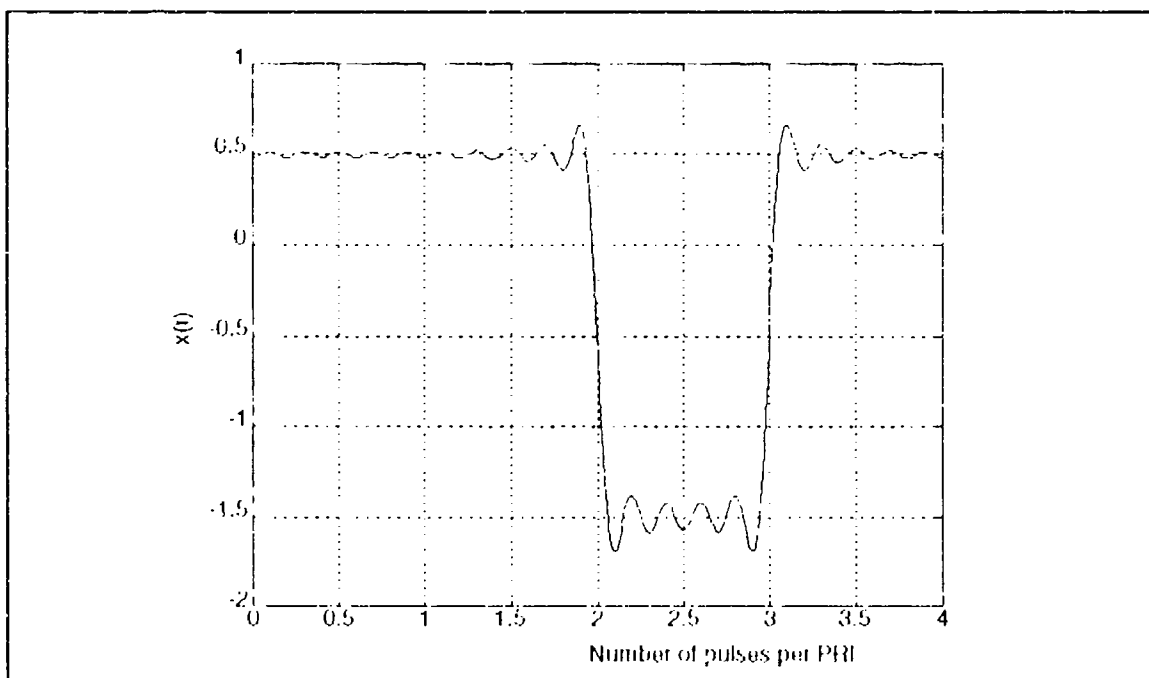Figure 4.13b   CW coded waveform (code + + - +), and
                PRF=0.25 GHz, ratio=1, N=20.

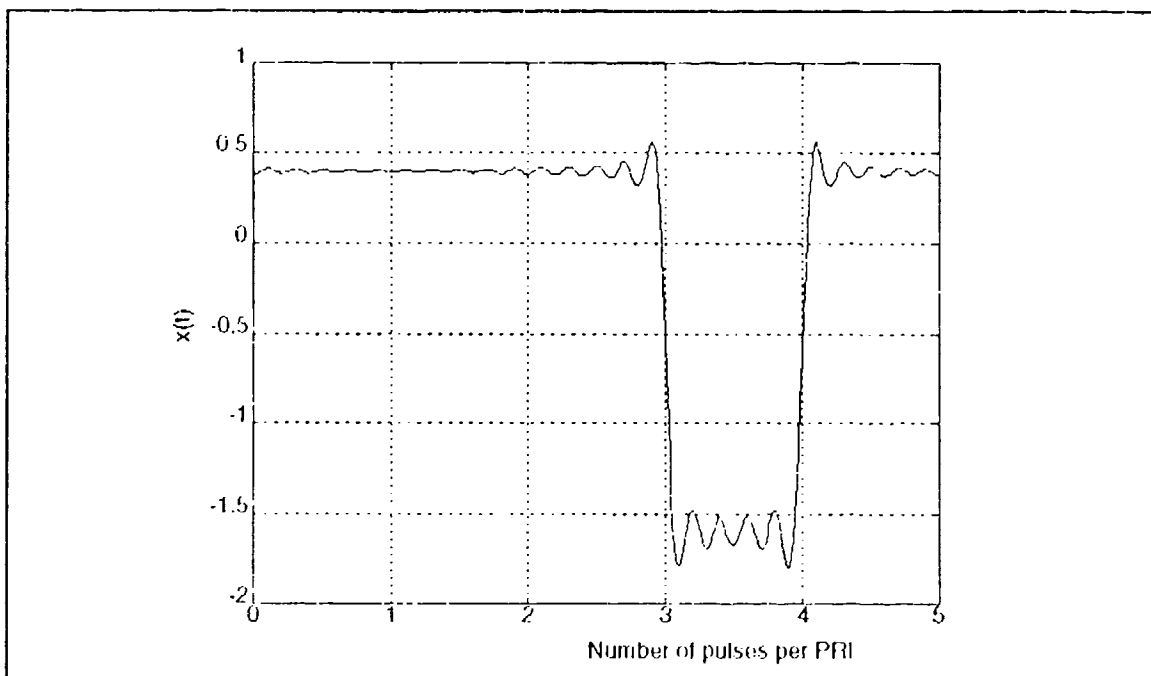Figure 4.13c   CW coded waveform (code + + + - +), and
                PRF=0.25 GHz, ratio=1, N=25.
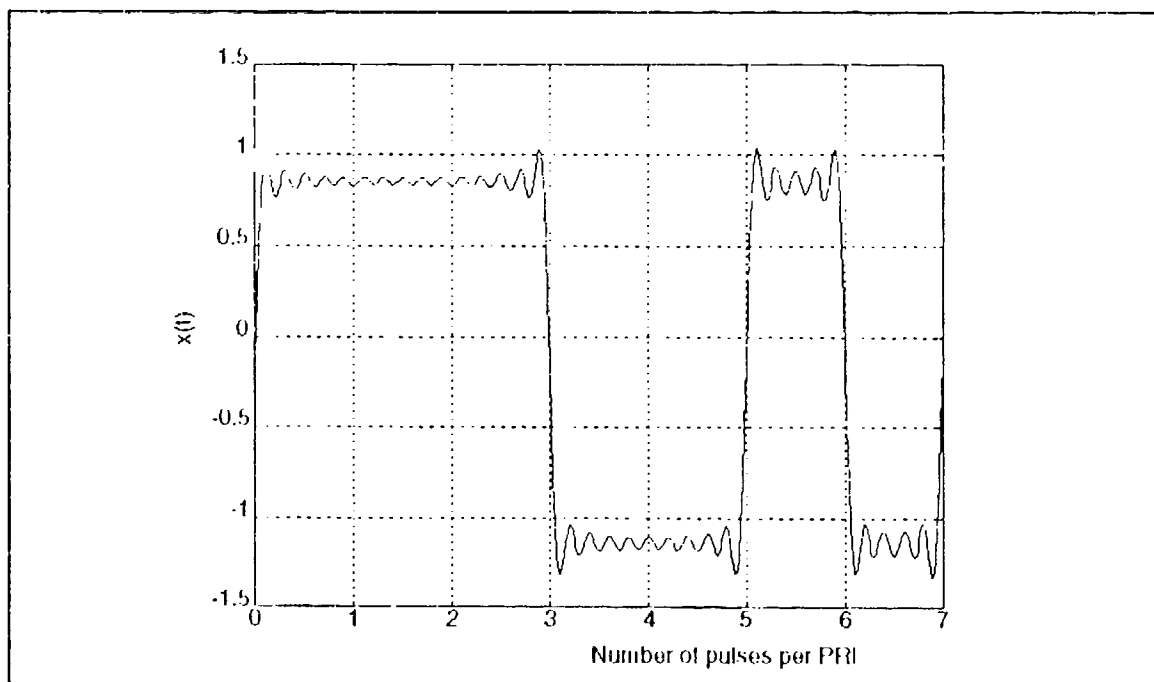

Figure 4.13d   CW coded waveform (code + + + - + - +), and
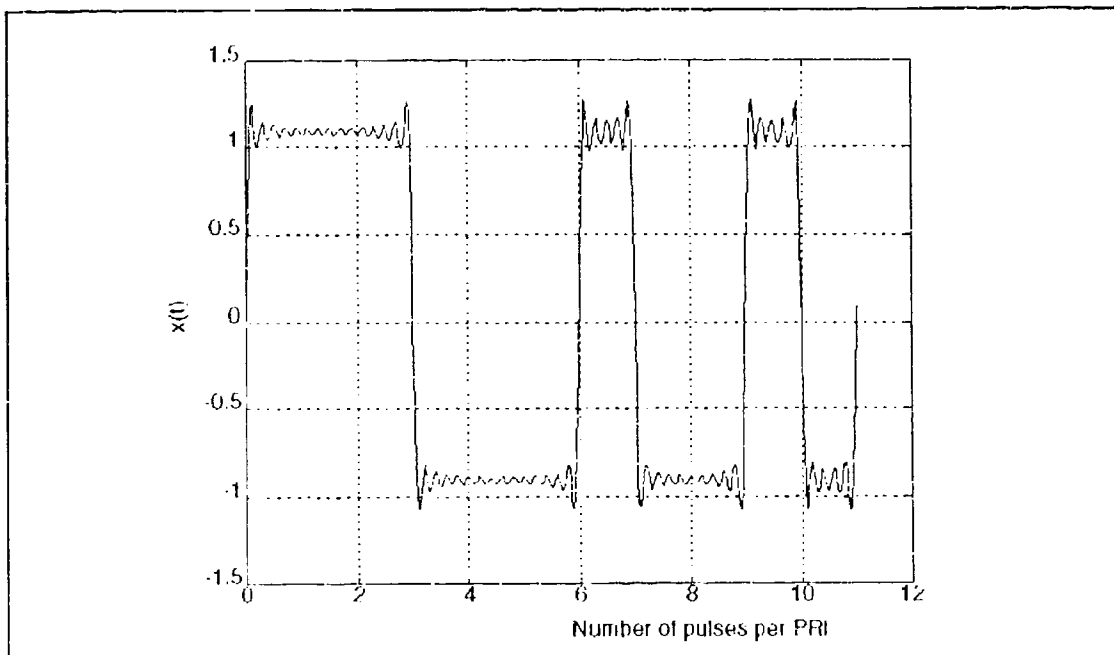   PRF=0.25 GHz, ratio=1, N=35.

Figure 4.13e   CW coded waveform (code +++---+--+-), and
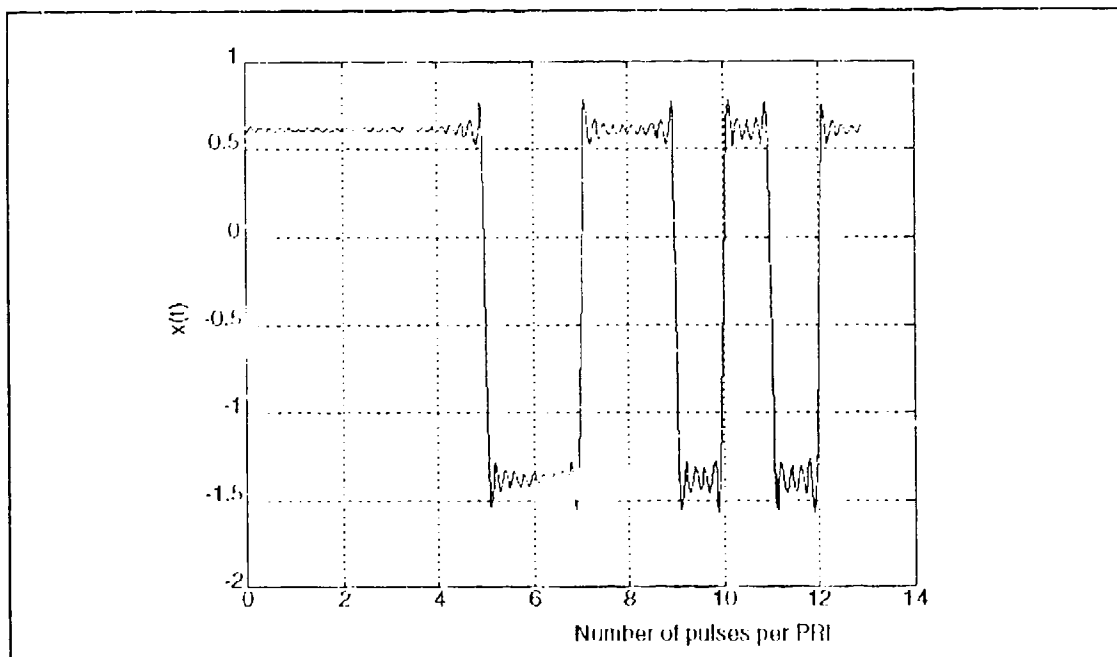   PRF=0.25 GHz, ratio=1, N=55.

Figure 4.13f   CW coded waveform (code +++++--+-+-+), and
                PRF=0.25 GHz, ratio=1, N=65.

The following examples illustrate the waveforms which are generated by different combinations as listed in Table (4.1).

TABLE 4.1   LIST OF PARAMETERS AND FIGURES FOR PULSED CODED WAVEFORM OF RATIO 5.

Fundamental PRF	Number of Subpulses per PRI	Code Length	Harmonics Used	Figure Number
0.25 GHz	15	3	9, 15, 64	4.14- a, b, c
0.25 GHz	20	4	9, 20, 64	4.15- a, b, c
0.25 GHz	25	5	9, 25, 64	4.16- a, b, c
0.25 GHz	35	7	9, 35, 64	4.17- a, b, c
0.25 GHz	55	11	9, 55, 64	4.18- a, b, c
0.25 GHz	65	13	9, 65, 81	4.19- a, b, c

From these figures, it can be noticed that for all the cases of figure (a) series, the number of harmonics used is nine, which is less than the number of subpulses per PRF, resulting in coded waveforms that are distorted and with pulses that are barely distinguishable. It turns out that in order to retain a useful shape of a coded pulse, the number of harmonics should not be less than the number of subpulses contained in the PRI, that is $N \geq$ "the number of subpulses contained in each PRI", as seen from the figure (b) series. The greater the number of harmonics used, the better the waveform shape will be, as seen in the figure (c) series. However, a greater number of harmonics imply a greater number of oscillators.

Figure 4.14a   Pulsed coded waveform (code + + -), and
                PRF=0.25 GHz, ratio=5, N=9.

Figure 4.14b   Pulsed coded waveform (code + + -), and
                PRF=0.25 GHz, ratio=5, N=15.

57

Figure 4.14c   Pulsed coded waveform (code + + -), and
                PRF=0.25 GHz, ratio=5, N=64.

Figure 4.15a   Pulsed coded waveform (code + + - +), and
                PRF=0.25 GHz, ratio=5, N=9.

Figure 4.15b   Pulsed coded waveform (code + + - +), and
                PRF=0.25 GHz, ratio=5, N=20.

Figure 4.15c   Pulsed coded waveform (code + + - +), and
                PRF=0.25 GHz, ratio=5, N=64.
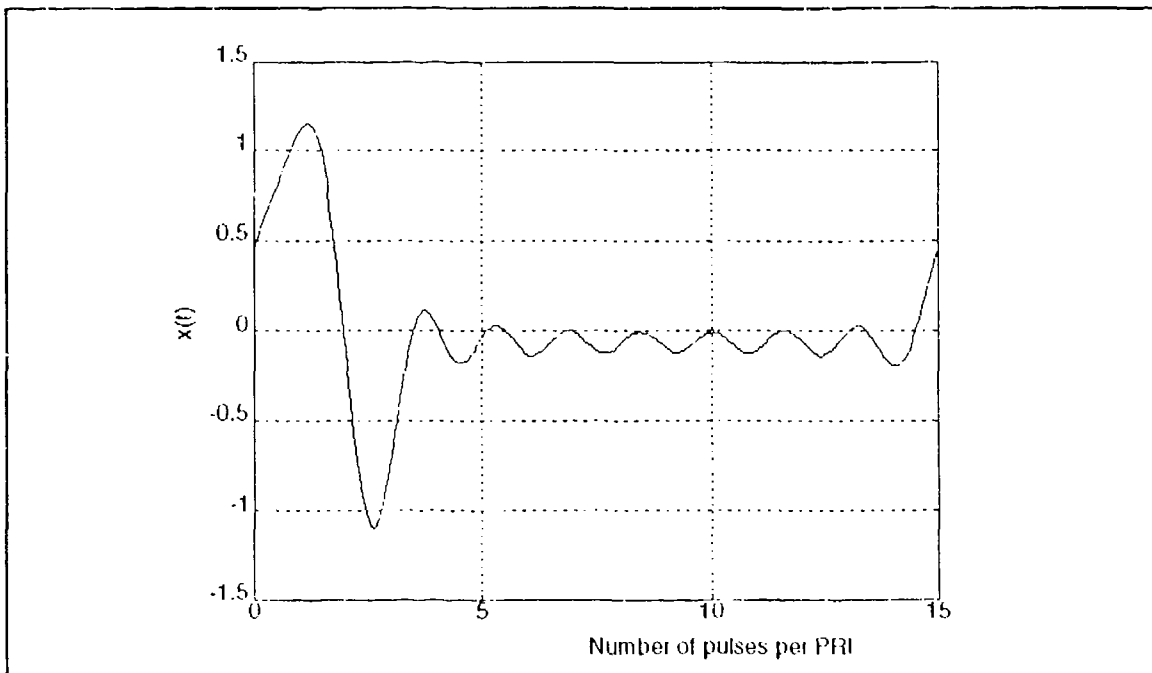
59

Figure 4.16a   Pulsed coded waveform (code + + + - +), and
                PRF=0.25 GHz, ratio=5, N=9.

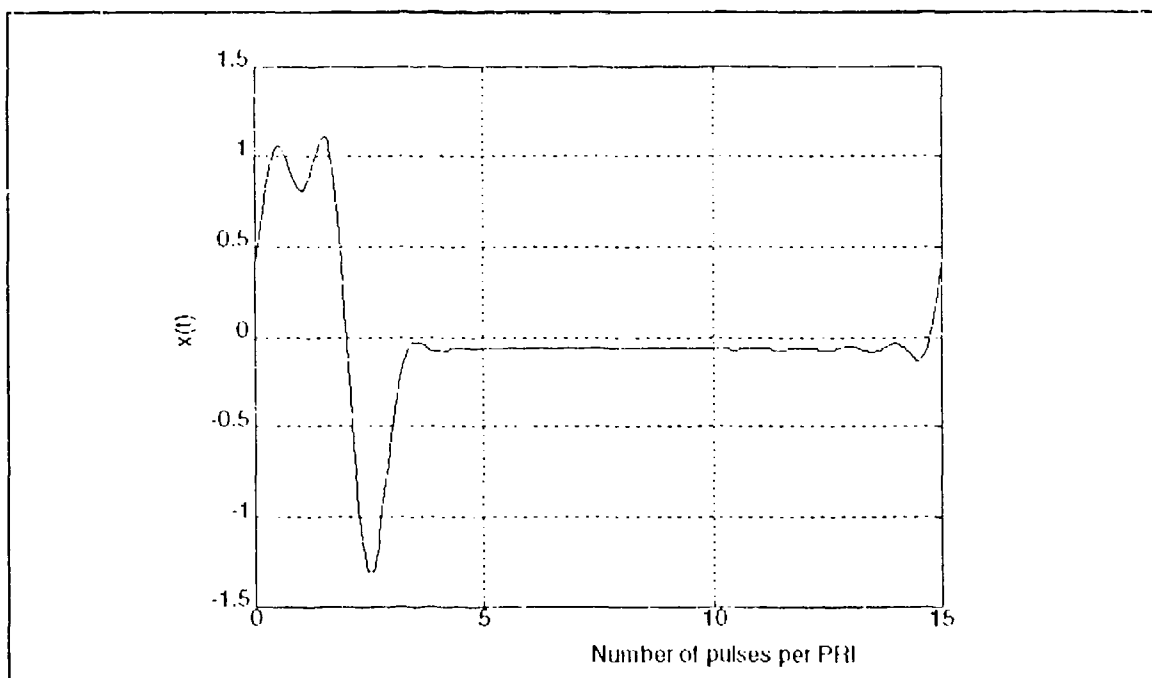Figure 4.16b   Pulsed coded waveform (code + + + - +), and
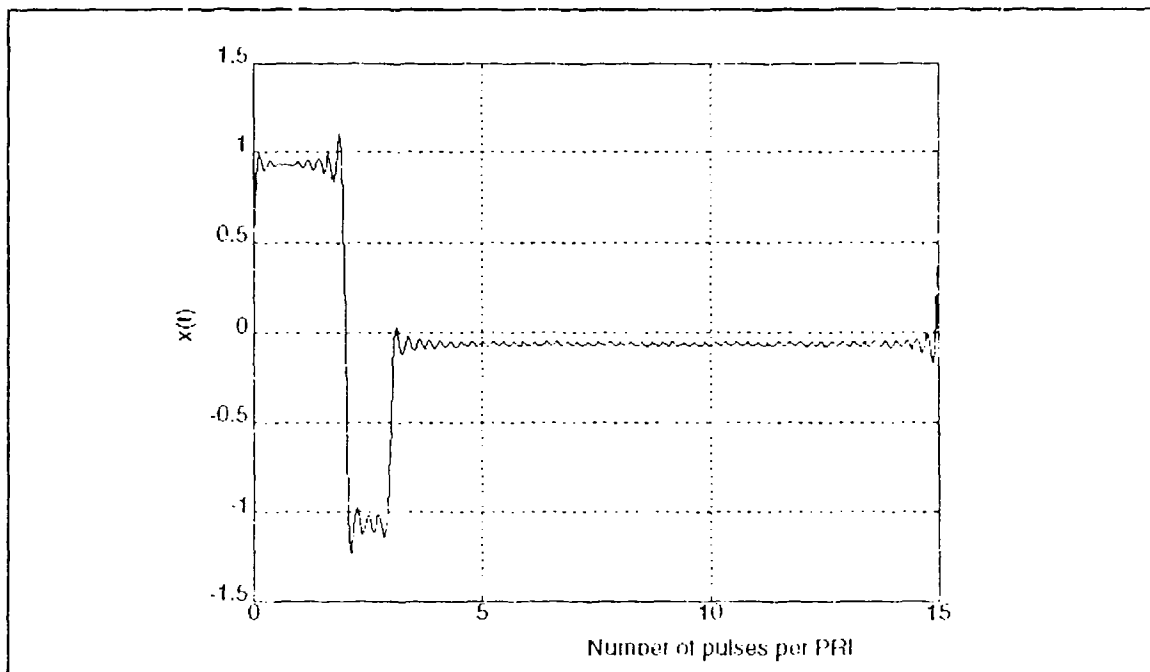   PRF=0.25 GHz, ratio=5, N=25.

Figure 4.16c   Pulsed coded waveform (code + + + - +), and
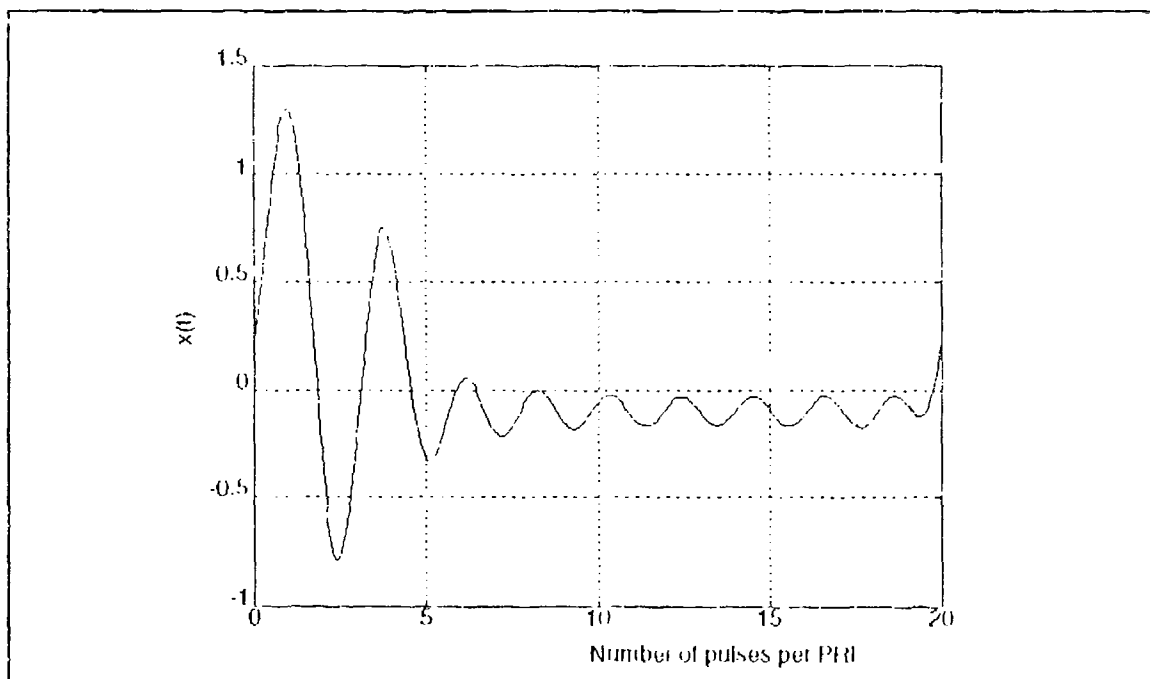   PRF=0.25 GHz, ratio=5, N=64.

Figure 4.17a   Pulsed coded waveform (code + + + - - + -),
                 and PRF=0.25 GHz, ratio=5, N=9.

Figure 4.17b   Pulsed coded waveform (code + + + - - + -),
                and PRF=0.25 GHz, ratio=5, N=35.

Figure 4.17c   Pulsed coded waveform (code + + + - - + -),
                and PRF=0.25 GHz, ratio=5, N=64.

Figure 4.18a   Pulsed coded waveform (code +++---+--+-), and
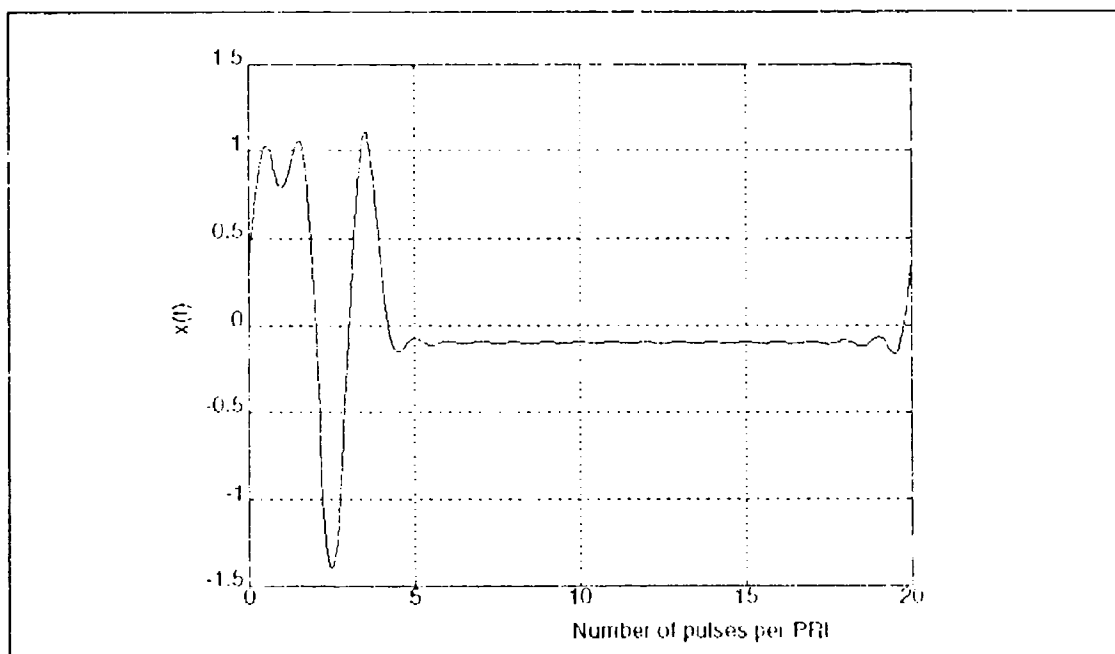PRF=0.25 GHz, ratio=5, N=9.

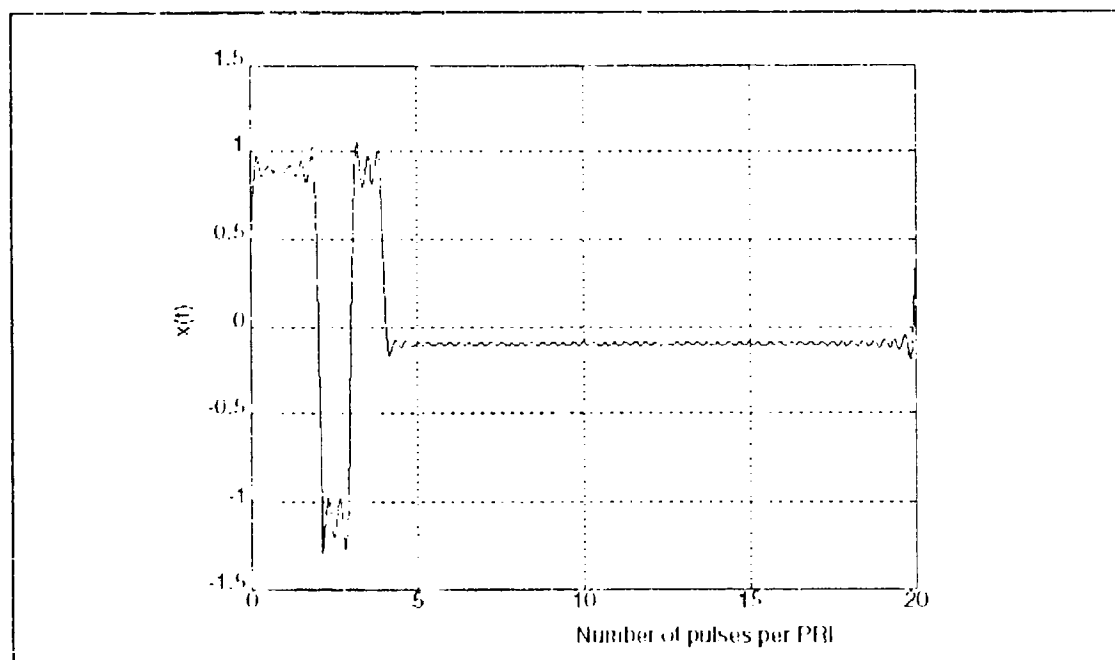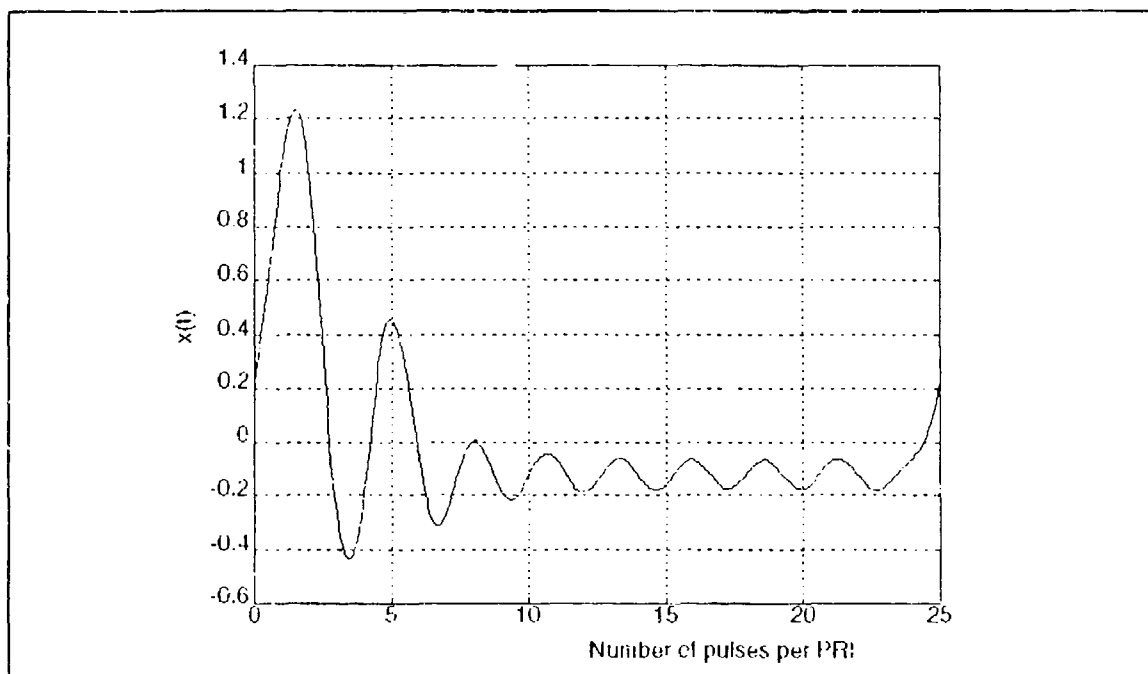Figure 4.18b   Pulsed coded waveform (code +++---+--+-), and
PRF=0.25 GHz, ratio=5, N=55.
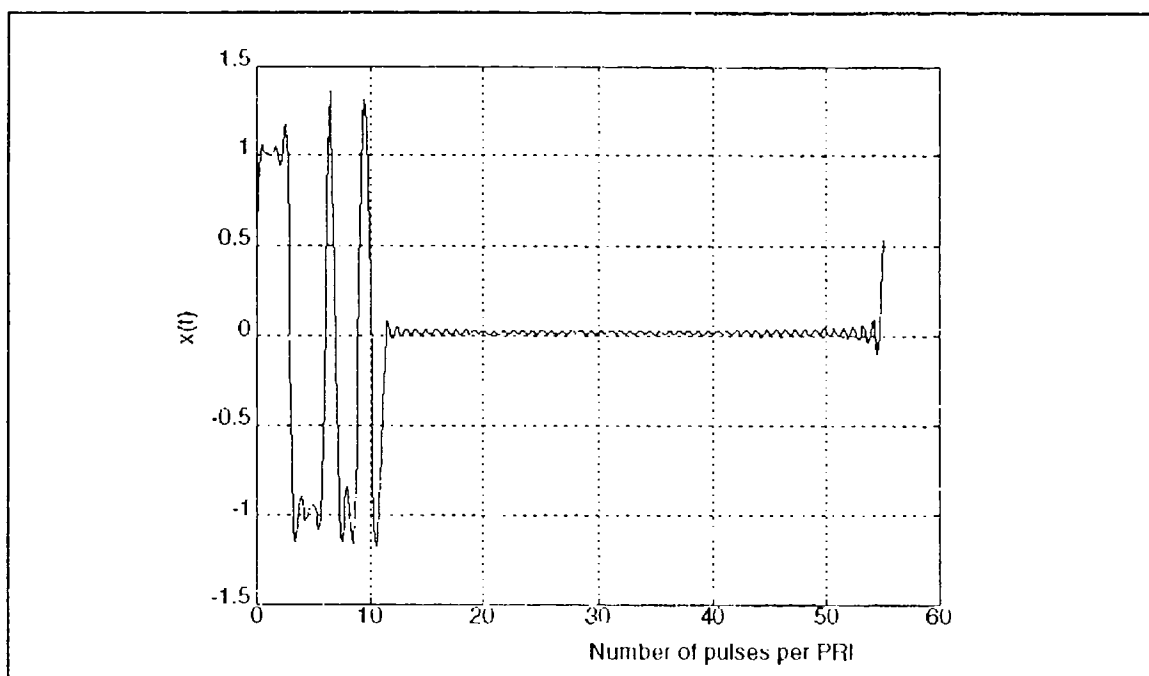
Figure 4.18c   Pulsed coded waveform (code +++---+--+-), and PRF=0.25 GHz, ratio=5, N=64.
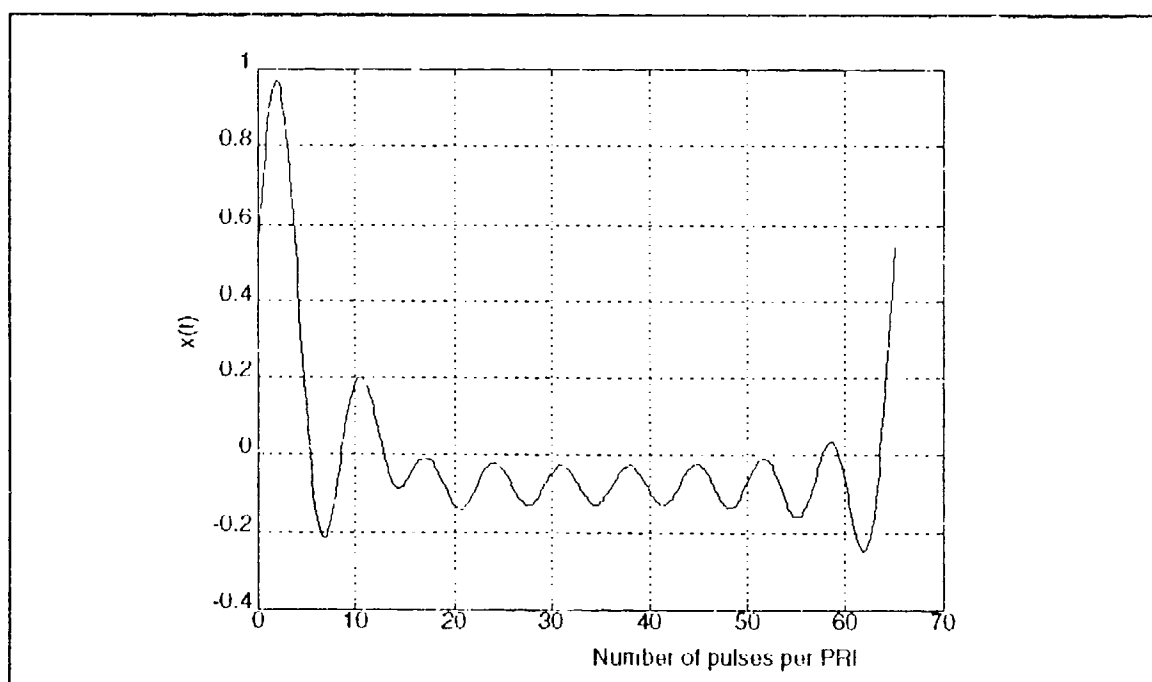
Figure 4.19a   Pulsed coded waveform (code +++++---++-+-+), and PRF=0.25 GHz, ratio=5, N=9.
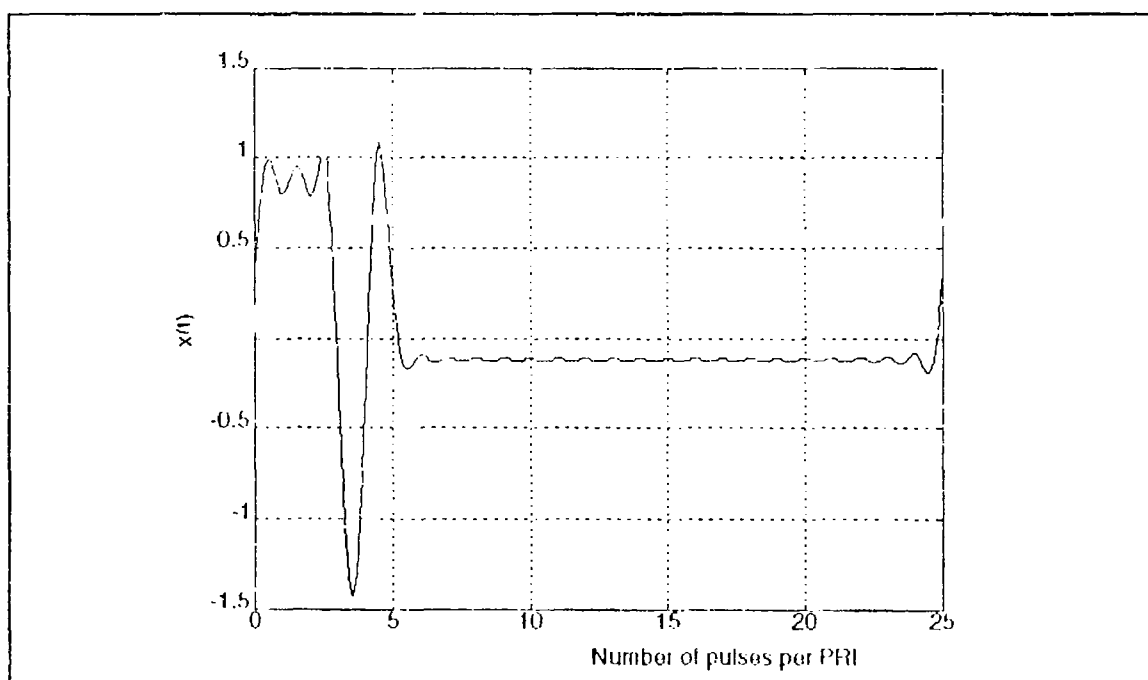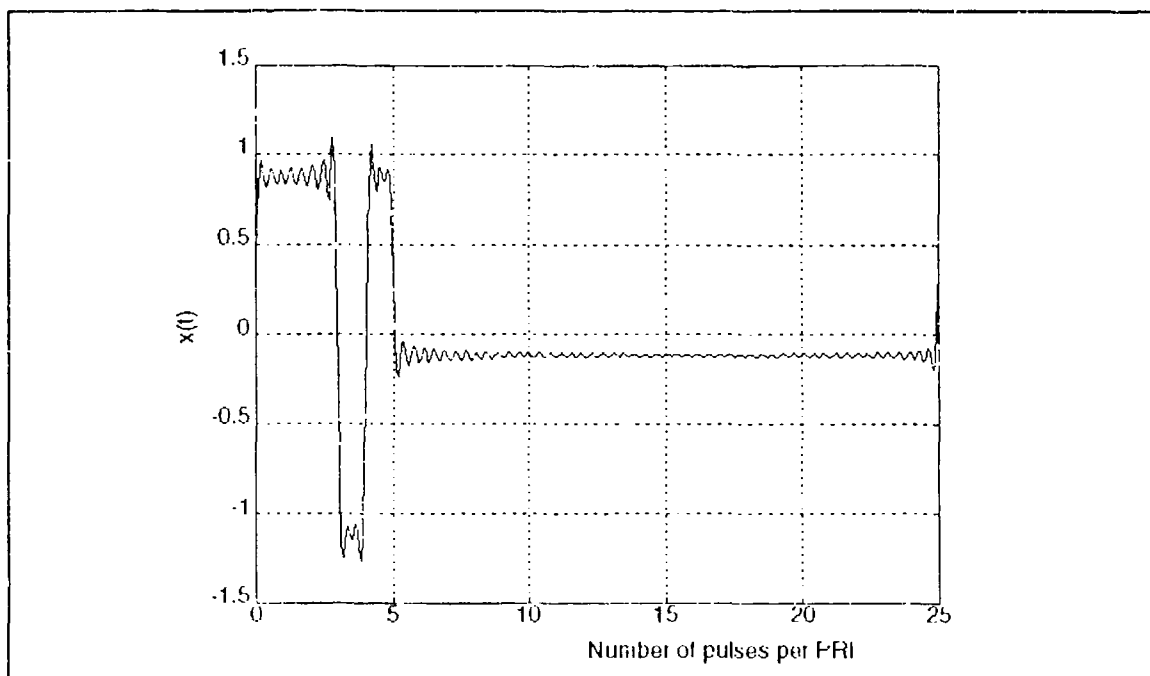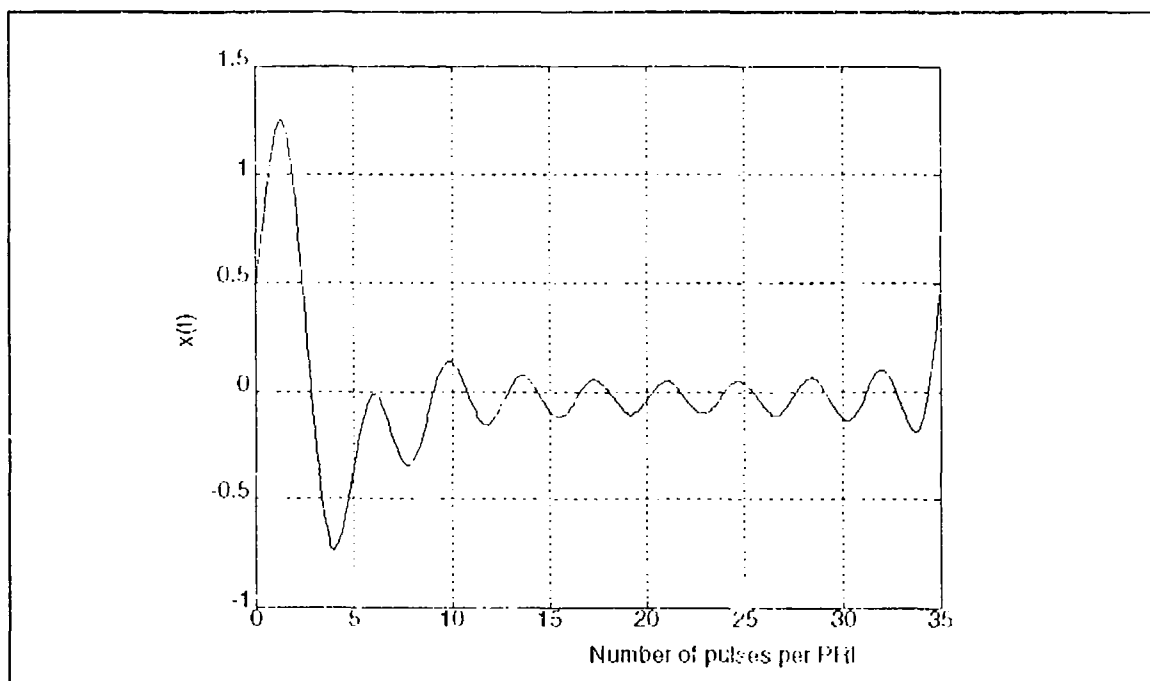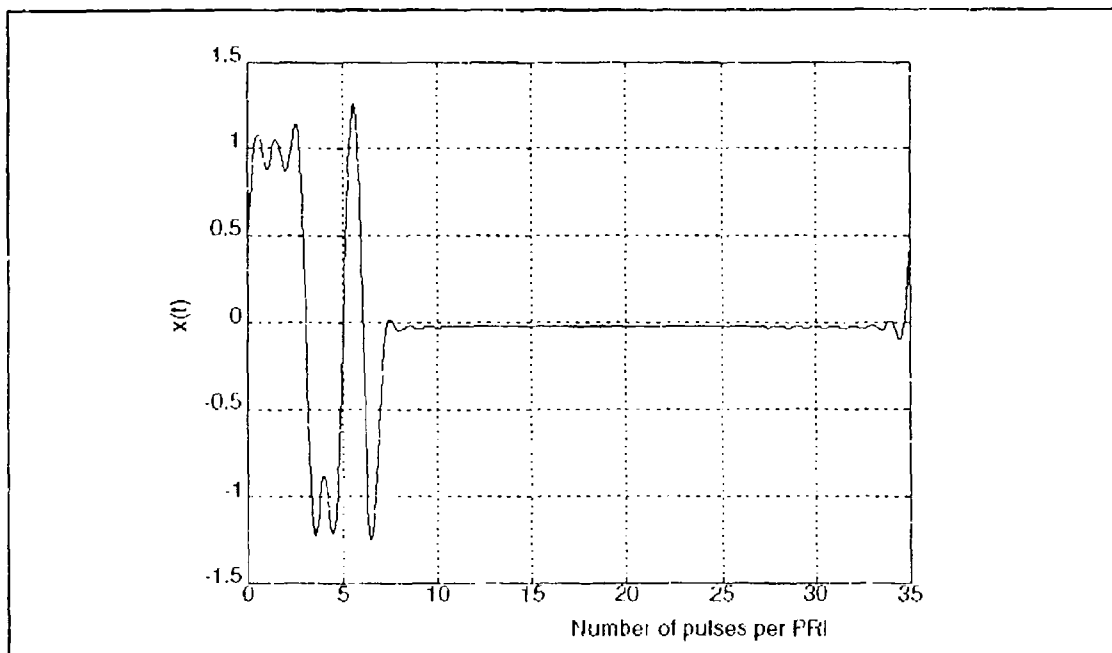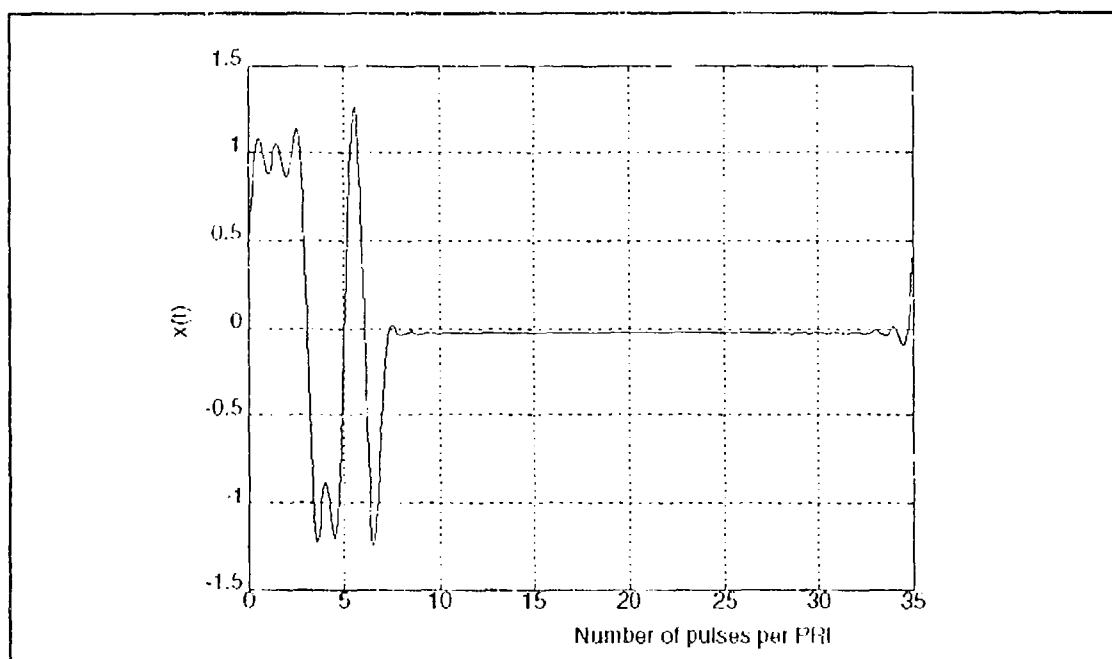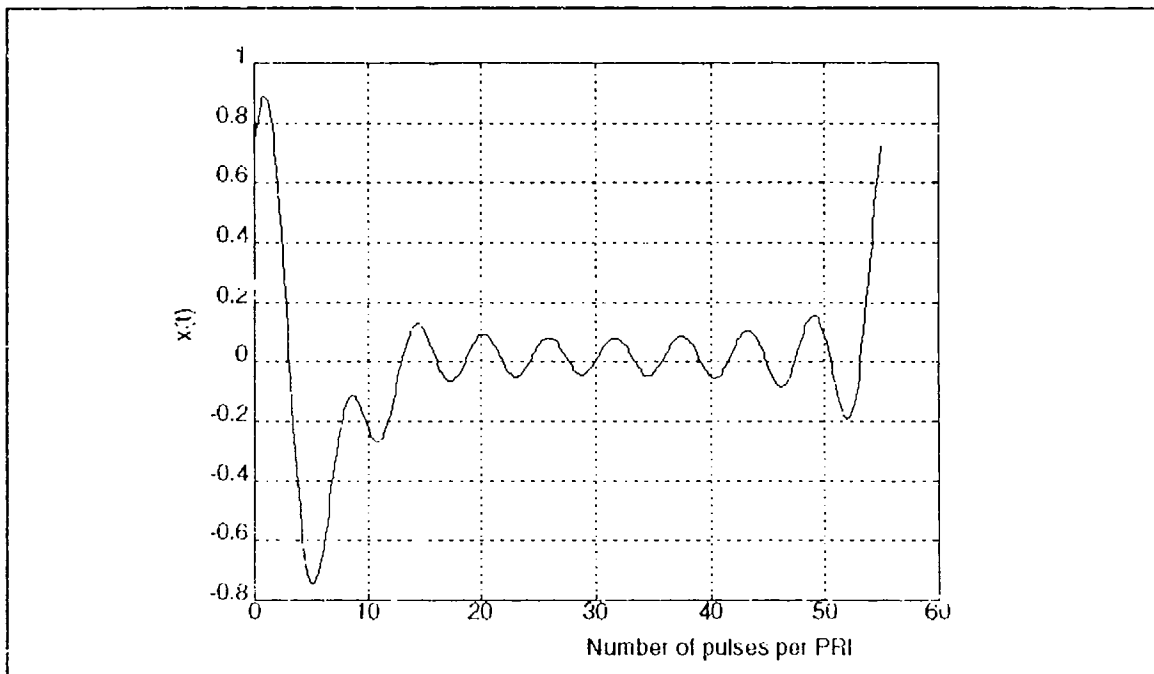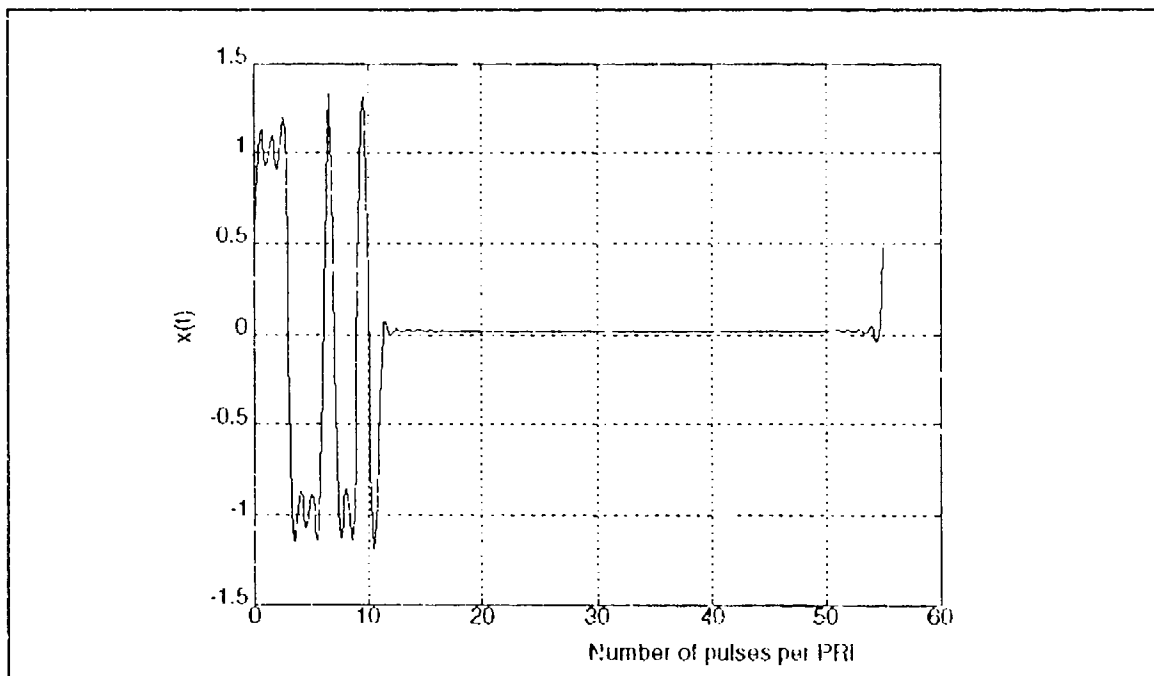
64
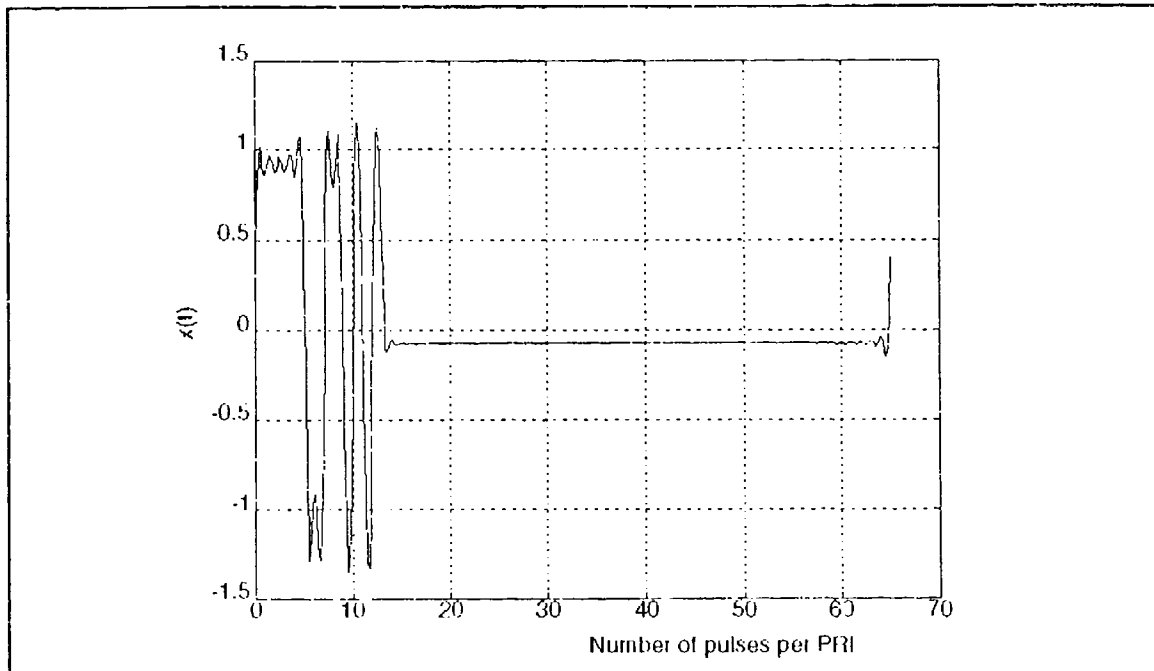
Figure 4.19b   Pulsed coded waveform (code ++++++--++-+-+),
                and PRF=0.25 GHz, ratio=5, N=65.
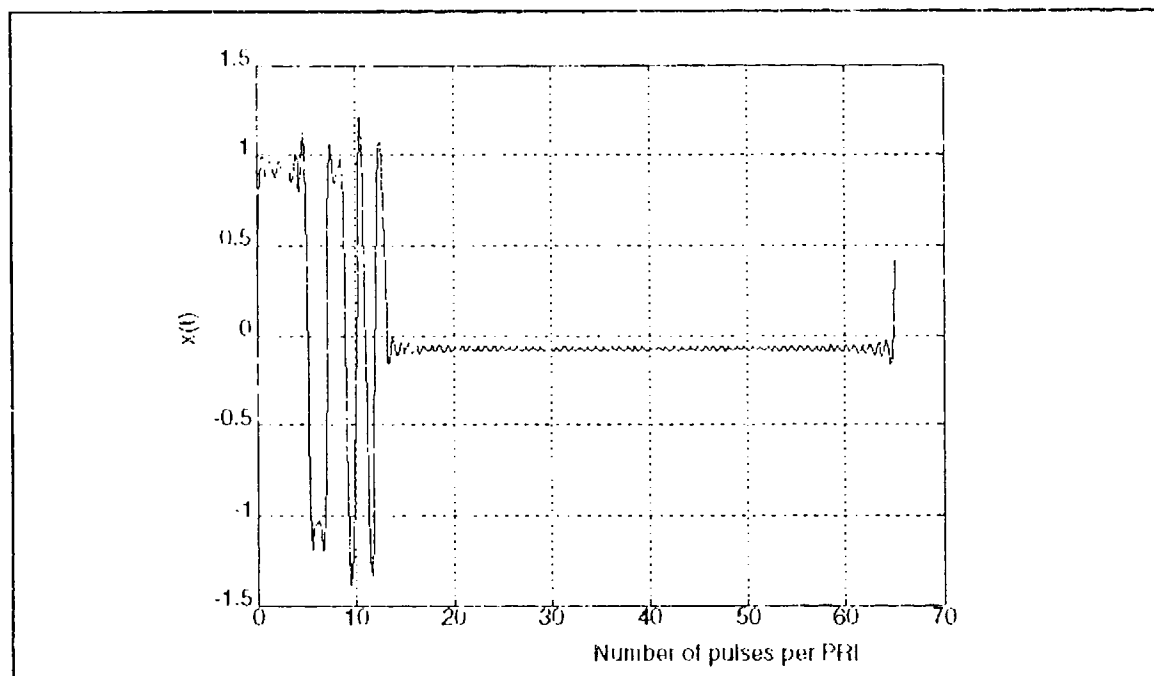
Figure 4.19c   Pulsed coded waveform (code ++++++--++-+-+),
                and PRF=0.25 GHz, ratio=5, N=81.

65

V. CONCLUSION

This thesis investigates the technologies for generation of high power, narrow pulse width baseband waveforms for UWB radar systems.

The traditional method of high power generation has been investigated over the years and results have been documented in the literature. The basic principle is the storage of energy by relatively low power sources followed by a sudden energy release to achieve high peak power in a short duration. Two popular types of switching devices and one energy storage device were reviewed. The problems of the traditional methods are: (1) low energy efficiency; (2) difficulty in controlling pulse shape; (3) maintaining accurate PRF, and; (4) avoiding interference to other friendly receivers. These problems limit their use in UWB system applications.

On the contrary, the Fourier synthesis method of generation has not been discussed in the literature. A Fourier series is normally used to analyze and decompose a signal $x(t)$ into a set of sinusoidal basis functions. However, a Fourier series can be used in reverse to synthesize $x(t)$ by generating and transmitting the individual sinusoidal components. Waveform synthesis is accomplished by coherently combining a discrete number of spectral lines, with each component generated by a separate source which is phase-locked to a master oscillator. The most unique feature of this method is

66

that the impulses are formed in space based on the Fourier synthesis in the frequency domain, rather than being produced by a single high power source in real time. Also the Fourier synthesis method spreads the burden of power generation over many signal sources, with each contributing only a fraction of the total power. This avoids the problem of high voltage breakdown as is often encountered in traditional methods and hence will ensure long term system stability. Other advantages are:

o   Instead of having a large single power source, it is possible to build pulse power by using many sources of lower power.

o   This method provides more accurate control of pulse parameters such as pulse shape and PRF. This advantage comes from the accurate phase control of phase-locked oscillators.

o   Interference to receivers can be avoided by suppressing a particular frequency without degrading the pulse shape too much. Conversely, outside interference to friendly receivers can be avoided by suppressing a return at a specific frequency.

o   It is possible to easily generate coded signals for pulse compression and increase the average power for better detection performance.

Two basic methods, "Fourier series" and "Sum of sinusoids" have been investigated in this thesis. Furthermore the Fourier series method also offers the possibility of coded waveforms using the built-in amplitude and phase control in each frequency channel. Coded waveforms are used in conventional narrow band radars to increase the average power (for higher detection performance) and still retain the advantages of shorter pulses. Average power is particularly

67

low in UWB waveforms due to its very narrow pulse width. Thus, it is all the more important to employ coded waveforms to increase the average power. In this thesis two methods of generation of coded waveforms are discussed. These are "continuous wave coded waveforms" and "pulsed coded waveforms". The continuous wave coded waveforms will repeat themselves indefinitely which is not of much utility for pulsed radars. Thus to have a pulse coded waveform with controlled PRF, switches must be employed. Oscillators are turned on for the length of coded pulse and then turned off to achieve the desired PRF. The pulsed coded waveforms can also be generated without using any switches, but it would require additional oscillators to maintain clear signal shapes. Thus, there is a tradeoff between switches and the number of oscillators used to achieve desired PRF. In general, the first method will be more efficient in most situations. It requires fewer oscillators and allows independent control of PRF and the lowest frequency component. The second method is suitable for very high PRF waveforms.

APPENDIX A   FOURIER SERIES EXPRESSION FOR THE
PERIODIC TRAIN OF UNIT IMPULSES

Consider a rectangular pulse train, as shown in Figure (4.1b). Each single rectangular pulse is defined as equation (4.6) but with unit pulse area, so the amplitude becomes $1/\tau$. The Fourier coefficients a_0 and a_n can be calculated by equation (4.2) and (4.10)

$$a_0 = \frac{2}{T} \int_{-\frac{T}{2}}^{\frac{T}{2}} x(t)\,dt = \frac{2}{T} \int_{-\frac{\tau}{2}}^{\frac{\tau}{2}} \frac{1}{\tau} \cdot dt = \frac{2}{T} , \qquad (A.1)$$

$$a_n = \frac{2A}{n\pi} \cdot \sin\left[\frac{nw_0\tau}{2}\right] = \frac{2}{n\pi\tau} \cdot \sin\left[\frac{nw_0\tau}{2}\right] . \qquad (A.2)$$

Due to an impulse, its pulse width is very small, then $\sin\theta$ can approximate θ

$$a_n = \frac{2}{n\pi\tau} \cdot \sin\left[\frac{nw_0\tau}{2}\right] \simeq \frac{2}{n\pi\tau} \cdot \frac{nw_0\tau}{2} \simeq \frac{2}{T} . \qquad (A.3)$$

Therefore the magnitude of a_n becomes independent of n. The spectrum then consists of an infinite series of lines with constant height and spacing.

From equations (4.1), (A.1) and (A.3), one can define the Fourier series expression of the periodic train of unit impulses

$\delta_T(t)$ as:

$$\delta_T(T) \ = \ \sum_{n=-\infty}^{\infty} \delta(t - nT) \ = \ \frac{1}{T} \ + \ \frac{2}{T} \cdot \sum_{n=1}^{\infty} \cos(nw_0 t) \ . \qquad (A.4)$$

70

APPENDIX B FOURIER COEFFICIENTS FOR CONTINUOUS WAVE
BARKER CODED WAVEFORMS

Using the same method described in section (IV.C.3.a), Fourier coefficients for "continuous wave coded waveforms" can be calculated as:

2-bit Barker code

$$a_n = \frac{A}{n\pi} \cdot \left[2\sin\frac{4n\pi}{2} - \sin\frac{6n\pi}{2} \right] , \qquad (B.1)$$

$$b_n = \frac{A}{n\pi} \cdot \left[1 - 2\cos\frac{4n\pi}{2} + \cos\frac{6n\pi}{2} \right] . \qquad (B.2)$$

3-bit Barker code

$$a_n = \frac{A}{n\pi} \cdot \left[2\sin\frac{4n\pi}{3} - \sin\frac{6n\pi}{3} \right] , \qquad (B.3)$$

$$b_n = \frac{A}{n\pi} \cdot \left[1 - 2\cos\frac{4n\pi}{3} + \cos\frac{6n\pi}{3} \right] . \qquad (B.4)$$

4-bit Barker code

$$a_n = \frac{A}{n\pi} \cdot \left[2\sin\frac{4n\pi}{4} - 2\sin\frac{6n\pi}{4} + \sin\frac{8n\pi}{4} \right] , \qquad (B.5)$$

$$b_n = \frac{A}{n\pi} \cdot \left[1 - 2\cos\frac{4n\pi}{4} + 2\cos\frac{6n\pi}{4} - \cos\frac{8n\pi}{4} \right) . \qquad (B.6)$$

5-bit Barker code

$$a_n = \frac{A}{n\pi} \cdot \left[2\sin\frac{6n\pi}{5} - 2\sin\frac{8n\pi}{5} + \sin\frac{10n\pi}{5} \right] , \qquad (B.7)$$

$$b_n = \frac{A}{n\pi} \cdot \left[1 - 2\cos\frac{6n\pi}{5} + 2\cos\frac{8n\pi}{5} - \cos\frac{10n\pi}{5} \right] . \qquad (B.8)$$

7-bit Barker code

$$a_n = \frac{A}{n\pi} \cdot \left[2\sin\frac{6n\pi}{7} - 2\sin\frac{10n\pi}{7} + 2\sin\frac{12n\pi}{7} - \sin\frac{14n\pi}{7} \right] , \quad (B.9)$$

$$b_n = \frac{A}{n\pi} \cdot \left[1 - 2\cos\frac{6n\pi}{7} + 2\cos\frac{10n\pi}{7} - 2\cos\frac{12n\pi}{7} + 2\cos\frac{14n\pi}{7} \right] .$$
$$(B.10)$$

11-bit Barker code

$$a_n = \frac{A}{n\pi} \cdot \left(2\sin\frac{6n\pi}{11} - 2\sin\frac{12n\pi}{11} + 2\sin\frac{14n\pi}{11} - 2\sin\frac{18n\pi}{11} \right.$$
$$\left. + 2\sin\frac{20n\pi}{11} - \sin\frac{22n\pi}{11} \right) ,$$
$$(B.11)$$

$$b_n = \frac{A}{n\pi} \cdot \left(1 - 2\cos\frac{6n\pi}{11} + 2\cos\frac{12n\pi}{11} - 2\cos\frac{14n\pi}{11} + 2\cos\frac{18n\pi}{11} \right.$$
$$\left. - 2\cos\frac{20n\pi}{11} + \cos\frac{22n\pi}{11} \right) .$$
$$(B.12)$$

13-bit Barker code

$$a_n = \frac{A}{n\pi} \cdot \left(2\sin\frac{10n\pi}{13} - 2\sin\frac{14n\pi}{13} + 2\sin\frac{18n\pi}{13} \right.$$

$$\left. - 2\sin\frac{20n\pi}{13} + 2\sin\frac{22n\pi}{13} - 2\sin\frac{24n\pi}{13} + \sin\frac{26n\pi}{13} \right) ,$$

$$(B.13)$$

$$b_n = \frac{A}{n\pi} \cdot \left(1 - 2\cos\frac{10n\pi}{13} + 2\cos\frac{14n\pi}{13} - 2\cos\frac{18n\pi}{13} \right.$$

$$\left. + 2\cos\frac{20n\pi}{13} - 2\cos\frac{22n\pi}{13} + 2\cos\frac{24n\pi}{13} - \cos\frac{26n\pi}{13} \right) .$$

$$(B.14)$$

LIST OF REFERENCES

1. Roger S. Vickers, *"Ultra-wideband Radar - Potential and Limitations,"* IEEE MTT-S Digest, 1991.

2. James D. Taylor, *"Ultrawideband Radar,"* US Air Force, Hanscom AFB, MA.

3. H. F. Harmuth, *"Nonsinusoidal Waves for Radar and Radio Communication,"* New York, Academic, 1981.

4. Harold F. Engler, Jr., *"An Assessment of Baseband Radar from A System Perspective,"* in *Ultra-Wideband Radar: Proceedings of The First Los Alamos Symposium*, Bruce Noel, editor, CRC press, Boca Raton, FL, 1991.

5. Merrill I. Skolnik, *"An Introduction to Impulse Radar,"* Naval Research Laboratory, Memorandum Report 6755, Washington, D.C., November 1990.

6. Lujing Cai, Hong Wang, *"Detection of Over-resolved Targets with the Range Migration,"* Proceeding International Conference on Radar, Peking, China, October 22-24, 1991.

7. Malek G.M. Hussain, *"An Overview of Developments in Nonsinusoidal-Wave Technology,"* IEEE International Radar Conference, 1985.

8. M. Abdullah and E. Kuffeland, *"High Voltage Engineering,"* Pergamon Press Ltd, Headington Hill Hall, Oxford, 1970.

9. C. Jerald Buchenauer, *"Spark Gap Generated Electromagnetic Pulses for Time Domain Measurements,"* in *Ultra-Wideband Radar: Proceedings of The First Los Alamos Symposium*, Bruce Noel, editor, CRC press, Boca Raton, FL, 1991.

10. J. A. Demarest, *"Frequency-agile Ultrawide Band Microwave Source,"* in *Ultrawideband Radar*, Ivan J. LaHaie, editor, proc. SPIE 1631, Bellingham, WA, 1992.

11. A. Kim, R. Youmans, and M. Weiner, G. Tran, L. Jasper, B. Lalevic, *"Monolithic, Photoconductive GaAs Pulser and Its Radiated Waveform,"* in *Ultrawideband Radar*, Ivan J. LaHaie, editor, proc. SPIE 1631, Bellingham, WA, 1992.

12. Ralph James, Howard Rhinehart, and Hardev Singh, *"Compact, High Voltage Modulator for Direct Radiation of Ultrawide Band RF Pulses,"* in *Ultrawideband Radar*, Ivan J. LaHaie, editor, proc. SPIE 1631, Bellingham, WA, 1992.

13. P. A. Pincosy, P. Poulsen, J.J. Morrison, *"Ultra-Wideband Generator,"* in *Ultrawideband Radar*, Ivan J. LaHaie, editor, proc. SPIE 1631, Bellingham, WA, 1992

14. David J. Mayhall, Jick H. Yee, and Raymond A Alvarez, *"High-Power Microwave Bandwidth Broadening by Air Breakdown,"* in *Ultrawideband Radar*, Ivan J. LaHaie, editor, proc. SPIE 1631, Bellingham WA, 1992

15. D. J. Mayhall, and J. H. Yee, *"Calculational Prediction of Ultrawide Band Electromagnetic Pulses by Laser-Initiated Air Avalanche Switches,"* in *Ultrawideband Radar*. Ivan J. LaHaie, editor, proc. SPIE 1631, Bellingham, WA, 1992

16. P. Van Etten, *"The Present Technology of Impulse Radars,"* in *Radar-77*, International conference, IEEE catagory number 77CH1271-6 AES, Page Bros (Norwich) Ltd. 1977.

17. M. Robert, *"Encyclopedia of Physical Science and Technology,"* Volume 11, Academic Press. Inc , 1987.

18. Raymond Tang, Kuan M. Lee, *"An Ultrawide Band Adaptive Transmitter for Ultrawide Band Radar Feasibility Demonstration,"* in *Ultrawideband Radar*, Ivan J. LaHaie, editor, proc. SPIE 1631, Bellingham, WA, 1992

INITIAL DISTRIBUTION LIST

1. Defense Technical Information Center   2
   Cameron Station
   Alexandria VA 22304-6145

2. Library code 52   2
   Naval postgraduate School
   Monterey CA 93943-5002

3. Chairman, Code EC   1
   Department of Electrical and Computer Engineering
   Naval Postgraduate School
   Monterey, CA 93943-5121

4. Dr. Gurnam S. Gill, Code EC/G1   4
   Department of Electrical and Computer Engineering
   Naval Postgraduate School
   Monterey, CA 93943-5121

5. Dr. Darvish Abdel Aziz Mohamed   1
   Air Defence College
   El Tabia, Alexandria, Egypt

6. Dr. J. Hall Code ONR 214   1
   Office of the Naval Research
   Ballston Tower 1, 800 N. Quincy Street
   Arlington, VA 22217-5660

7. Library   1
   Chung Cheng Institute of Technology
   P.O. Box 90047, Ta-Hsi, Tao-Yuan
   33500, Taiwan R.O.C.

8. Library   1
   Naval Academy
   P.O. Box 90175, Tso-Ying,
   Kao Hsiung. Taiwan, R.O.C.

9. Tsann. N.C. Yao PhD.   1
   #-50 Kwung, Fu S. Road
   Apt. #2 on 10th Floor
   Taipei, Taiwan, R.O.C.

10. CDR. Chiang Hsiao Feng   1
    #137-1 King Hwa Street
    Taipei, Taiwan, R.O.C.